High order invariant manifold model reduction for systems with non-polynomial non-linearities: geometrically exact finite element structures and validity limit

Aurélien Grolet, Alessandra Vizzaccaro, Marielle Debeurre, Olivier Thomas

High order invariant manifold model reduction for systems with non-polynomial non-linearities: geometrically exact finite element structures and validity limit

Aurélien Grolet, Alessandra Vizzaccaro, Marielle Debeurre, Olivier Thomas
Please send all correspondence to : aurelien.grolet@ensam.eu

June 7, 2024

Abstract

This paper considers the computation of reduced-order models for systems of ordinary differential equations that include non-polynomial non-linearities. An targeted example is the case of a geometrically exact model of highly flexible slender structure, that includes, after space discretisation, trigonometric nonlinear terms. With a suitable change of variables, this system can be rewritten in an equivalent one with polynomial nonlinearities at most quadratic, at the price of introducing additional variables linked to algebraic equations, leading to a differential algebraic set of equations (DAE) to be solved. This DAE is reduced thanks to a normal form parametrisation of its invariant manifolds and selecting a set of master ones. Arbitrary order expansions are detailed for the coefficients of the change of variable and the reduced dynamics, using linear algebra in the space of multivariate polynomials of a given degree. In the case of a single nonlinear mode reduction, a criterion to evaluate the quality of the normal form results is also proposed based on an estimation of the convergence radius of the polynomial asymptotic expansion representing truncated series. The method is then applied to compute a single mode reduction of three test cases – a Duffing oscillator, a simple pendulum and a clamped clamped beam with von Kármán model –, in order to investigate the effect of the algebraic part of the DAE on the quality of the model reduction and its validity range. Then, the more involved case of a cantilever beam modelled by geometrically exact finite elements is considered, underlining the ability of the method to produce accurate and converged results in a range of amplitude that can be bounded thanks to a convergence criterion.

1 Introduction

This paper considers the computation of reduced-order models for systems of ordinary differential equations (ODEs) that include non-polynomial nonlinearities. The main application cases are geometrically exact models of nonlinear slender structures discretised in space by a finite-element procedure, leading to differential equations that include sine and cosine trigonometric functions. The investigated reduction strategy consists in replacing the ODEs by an equivalent differential algebraic set of equations (DAE) with at most quadratic nonlinear terms and reducing its dynamics on a few invariant manifolds of the phase space using a normal form technique.

The concept of normal forms originates with the work of Poincaré [1] where the idea is, in a nutshell, to use a nonlinear change of variable to transform the original dynamics into a new one that has a simpler form and that can be solved more easily. The change of variable somehow absorbs the nonlinearity, leading to a new dynamics being linear in the best case. However, if the initial system has so-called resonance conditions, the new dynamics will always contain some nonlinear terms called the resonant terms: the new dynamics is still nonlinear, but simpler than the original one thanks to invariance properties. This properties also naturally lead to reduce the dynamics by selecting only a subset of master (normal) variables, associated to a reduced dynamics, the change of variables enabling to recover the initial variables in terms of the reduced set of normal variables. Additional details about the theoretical framwork of the normal form theory can be found in [2, 3, 4, 5, 6].

The present invariant manifold reduction technique is linked to the nonlinear normal mode concept, that extends the (linear) eigenmode definition to the nonlinear range. It is similar: one selects a reduced set of master coordinates that enable to efficiently compute the dynamics around a given resonance. For a conservative system in free vibrations, a NNM is defined equivalently as an invariant manifold of the phase space [7, 8, 9] or a family of periodic solutions [10, 11], also known as a Lyapunov subcenter manifold [12, 13, 14]. With dissipation included in the model, the invariant manifold definition still holds [15, 9] and coexists with other concepts [16, 17]. Historically, the concept of NNM / invariant manifold has been first proposed and tested on models of systems with a few degrees of freedom (either toy mass-spring models [18, 8, 11] or structures expanded

on a few linear modes [19, 20]) and its only recently that large finite-element discretised models of structures have been addressed without the preliminary modal expansion step to diagonalise the linear part [21]. This leaded to several software packages [22, 23] able to reduce the dynamics in free vibrations with possible internal resonances [24, 25, 26, 26, 27, 28, 29], but also in forced vibrations around primary and secondary resonances in direct and parametric forcing [30, 31, 32]. The present use of the normal form technique to compute the invariant manifold and the reduced dynamics is one choice among others, another one being the so-called graph style [21, 33, 34, 35, 36], used by Shaw & Pierre in the seminal work about NNM defined as invariant manifolds [7, 37]. A review of model reduction for geometrically nonlinear structures can be found in [21] with more recent references in [32, 38]. Some works also considers application to nonlinear PDE solved with the finite element method [39]. .

In this work, we assume that the initial dynamics can be written under the form of a quadratic differential algebraic equations (DAEs). Considering a quadratic DAE system offers a formalism that allows to easily express asymptotic expansions analytically and simplifies the writing of the normal form associated computations. Though being considered restrictive at first sight, it is possible to find an equivalent quadratic DAE to a given ODE system that contains any classical elementary transcendental functions (exp, log, sin, cos, power...), at the price of introducing new variables, as explained in [40, 41, 42]. DAEs are for example the starting formalism of the Manlab numerical continuation package that uses the asymptotic numerical method on quadratic DAE to compute their solutions as a parameter is varied [43], or can be used for time integration [44]. Considering the computation of reduced-order models for DAE using invariant manifolds has been considered recently in [45] with the spectral submanifold framework. However, in this work the authors transform the DAE into an ODE by taking the derivative of the algebraic equation with relation to time as many times as necessary. In the present work, the quadratic DAE is kept as such during all the procedure for the normal form computation. Moreover, using a quadratic DAE as a starting point for invariant manifold reduction has also been considered recently in [32] to treat the case of systems forced in the vicinity of a secondary resonance, with no emphasis on the effect of the algebraic part of the system on the model reduction, which is especially one of the goal of the present work.

In this paper, we propose a method to compute a reduced-order model of an autonomous quadratic DAE using a polynomial change of variable, a reduced dynamics and a normal form style for the parametrisation of the invariant manifold. The computations are carried out using linear algebra in the space of polynomials, allowing to express multiplication and derivation operations with matrices with a particular block structure. The equation to be assembled to compute the normal form at a given degree can then be easily assembled, avoiding tedious handwritten and/or symbolic computations and facilitating its numerical implementation up to an arbitrary polynomial order for the change of variables and the reduced dynamics.

The application of the method concerns in particular nonlinear mechanical systems modeled by the finite-element method with any type of nonlinearity, provided a quadratic recast can be found, thus including algebraic equations linked to the introduction of additional variables and/or constraints. A typical example is pendulum-like equations, that involve sine functions in the nonlinearity, or more generally, geometrically exact beam models where one has to take into account the displacement and the rotation of the cross section [46]. This is in contrast with the test cases of cantilever beams discretised with 3D finite-element presented in [27, 29], where only quadratic and cubic nonlinearities have to be considered since the finite-element degrees of freedom are only displacements and no cross section rotations. Additional applications concern electrical systems and power networks where machine dynamics and power balance appear naturally as quadatic DAEs [47].

As the normal form is an asymptotic expansion, it usually starts to diverge at high amplitudes and it can be useful to have validity bounds for the reduced model. Criteria have been proposed for the normal form in [48] and recent developments involve interesting discussions on the validity range of the different styles of parametrisations [49]. In this paper, we propose a simple validity limit estimation for single mode reduced-order models based on the d'Alembert and Cauchy criterion for convergence testing of power series.

The outline of the paper is as follows: first the proposed method and formalism are described in Section 2. Then a detailed application on a Duffing oscillator is given in Section 3. Section 4 considers the application of the proposed method to a simple pendulum system with various forms of parametrisations. Next, a simplified model of a clamped clamped beam is studied in Section 5. Finally, Section 6 shows the applicability of the proposed method by considering a cantilever beam discretised with geometrically exact finite-elements. The paper ends with some concluding remarks.

2 Description of the normal form computation

2.1 Definition of the formalism

In this paper we consider autonomous and conservative dynamical systems that can be represented by an autonomous quadratic DAE written under the following form:

$$A\dot{y} = Ly + Q(y, y) \tag{1}$$

where $y \in \mathbb{R}^N$ is the vector of dynamical variables, L a linear operator (constant $N \times N$ matrix with real coefficients) and A a (possibly singular) linear operator (constant $N \times N$ matrix with real coefficients). Q is a quadratic operator (vector of bilinear forms of size N) and $\dot{\circ} = \mathrm{d} \circ /\mathrm{d}t$ is the time derivative operation.

The vector of degrees of freedom $y(t)$ contains the state variables of the system (usually positions and velocities) along with Lagrange multipliers (if the dynamical system has constraints) and/or auxiliary variables needed to recast the original dynamics under a quadratic DAE, that may bring singularities in A because of the added algebraic equations. Although this formalism seems restrictive at first glance, it can actually account for many nonlinear systems and allows to carry analytical development further as explained in the introduction. This formalism is in particular used in the Manlab package as an input to compute periodic solutions using a combination of the harmonic balance method and the asymptotic numerical method [43].

In the remainder of the paper, we assume that the origin $y = 0$ is an equilibrium point (i.e. $Q(0, 0) = 0$), and we study the dynamics around that point. If this is not the case, then the procedure described in Appendix A can be used.

2.2 Linear eigenmodes

The (right) linear eigenmodes of the quadratic DAE are defined by the solution of the following eigenvalue problem:

$$(\lambda A - L)Y = 0 \tag{2}$$

where λ are the complex eigenvalues (possibly infinite due to the algebraic equations in the DAE) and Y the (right) complex eigenvectors (mode shapes). These eigenmodes are used for the linear part of the change of variable appearing in the normal form computation. Similarly, the (left) linear eigenmodes are defined by:

$$X^T(\lambda A - L) = 0 \tag{3}$$

where X represent a left eigenvectors. Those (left) eigenmodes are used as projectors during the normal form computation in the case of internal resonance. Note that since the operators L and A are real, the spectrum will contain only real or complex conjugated eigenvalues. Note that if the operator A is singular, then (real) infinite eigenvalues will appear in addition to the classical spectrum. These eigenvalues are associated with the algebraic equations that can be identified as constraints on the variables of the systems.

2.3 Normal form strategy

2.3.1 Normal form parametrisation

We consider an autonomous quadratic DAE in the form of Equation (1). In the normal form computation, we aim to find:

- (i) a nonlinear change of variable $y = W(z)$, where W is a columns vector whose components are polynomials (N components).
- (ii) a reduced nonlinear dynamics $\dot{z} = f(z)$, where f is a columns vector whose components are polynomials (n components) which we would like to be *as simple as possible* (i.e. containing as few terms as possible)

The variables in y are expressed as a function of the new variable $z = (z_1, z_2, ..., z_n)$ called complex normal variables. The invariant manifold is parametrised using the normal form style parametrisation [36, 33], which is contained in the change of variable $y = W(z)$.

For a complete normal form computation (no reduction), the variable in z should be associated to all pairs of complex conjugated eigenvalues of the linear eigenproblem in Equation (2), and in this case the computation is equivalent to computing the Poincaré-Birkhoff normal form [50].

In this paper, we consider model order reduction, therefore the reduced normal variable z will contain elements associated to selected pairs of complex conjugated eigenvalues of the linear problem. In the case of a single mode reduction, the variables z contains only two elements $z = (z_1, z_2)$.

In order to find an explicit expression for the change of variable $W(z)$ and the reduced dynamics $f(z)$, we use multivariate polynomials in the variable z up to a given degree D. $W(z)$ and $f(z)$ can then be defined by their coefficients matrix W and f relative to a monomial basis. In order to find the coefficients of the polynomials, we substitute the polynomial expansion into the original DAE (1), and we balance the coefficients of each monomial in order to obtain a set of equations defining the coefficients W and f. The remainder of the sections describes this procedure in detail.

2.3.2 Polynomial representation

The representation of the change of variable $W(z)$ and the reduced dynamics $f(z)$ uses multivariate polynomials of the variable z. In the aim of computing a normal form up to a given degree D, we consider the space of polynomials of degree D in n variables $z = (z_1, z_2, \ldots, z_n)$ with complex coefficients, denoted $\mathbb{C}_D[z]$. It is a vector space (over $\mathbb{C}$) with dimension $M = \frac{(D+n)!}{D!\ n!}$, and we introduce the (canonical) monomial basis $B(z)$ composed of the elementary monomials $b_m(z) = z^{\alpha_m} = z_1^{\alpha_{m1}}\ z_2^{\alpha_{m2}}\ \cdots\ z_n^{\alpha_{mn}}$, with $\alpha_m = (\alpha_{m1}, \ldots, \alpha_{mn}) \in \mathbb{N}^n$ such that $\sum_{k=1}^{n} \alpha_{mk} \leq D$, for $m \in [0,\ M-1]$:

$$B(z) = [b_0(z),\ b_1(z), \ldots, b_n(z), \ldots, b_{M-1}(z)]^T \tag{4}$$

The elements of the monomial basis are sorted by increasing total degree. In particular, we set $b_0(z) = 1$ (constant monomial), $b_1(z) = z_1$, $b_2(z) = z_2$, ..., and $b_n(z) = z_n$ (linear monomials).

A polynomial $\lambda(z) \in \mathbb{C}_D[z]$ will be written using its coordinates relative to the basis $B(z)$ as:

$$\begin{aligned} \lambda(z) &= \lambda_0 + \lambda_1 z_1 + \cdots + \lambda_n z_n + \lambda_{n+1} z_1^2 + \cdots + \lambda_m z_1^{\alpha_{m1}}\ z_2^{\alpha_{m2}}\ \cdots\ z_n^{\alpha_{mn}} + \cdots + \lambda_{M-1} z_n^D \\ &= \sum_{m=0}^{M-1} \lambda_m b_m(z) = \lambda B(z) \end{aligned} \tag{5}$$

where $\lambda = [\lambda_0,\ \lambda_1,\ \ldots,\ \lambda_{M-1}]$ is the (row) vector of coefficients for the polynomial $\lambda(z)$ relative to the basis $B(z)$.

Next, we consider $W(z)$ a (column) vector of N polynomials, whose components are denoted $W^j(z)$ for $j \in [1,\ N]$. Using the basis $B(z)$, we can identify the vector of polynomials $W(z) \in \mathbb{C}_D^N[z]$ with an $N \times M$ matrix of complex coefficients, denoted $W \in \mathcal{M}_{N\times M}(\mathbb{C})$, such that:

$$W(z) = W\ B(z) = \sum_{m=0}^{M-1} W_m b_m(z) = (W_0,\ W_1,\ W_2,\ \ldots,\ W_{M-1}) \begin{pmatrix} b_0(z) \\ b_1(z) \\ b_2(z) \\ \vdots \\ b_{M-1}(z) \end{pmatrix} \tag{6}$$

where $W_m \in \mathbb{C}^N$ is the vector of coefficients associated to the monomial $b_m(z)$ and also corresponds to the $m+1$ column of the matrix of coefficients W. The elements of the table of coefficient W are denoted $W_m^j \in \mathbb{C}$, where the subscript (m) refers to the monomial basis and the superscript (j) refers to the component of the vector $W(z)$. Using this notation, W_m is a column vector containing the coefficients associated to the monomial b_m and W^j is a raw vector containing all the coefficients for the polynomial $W^j(z)$.

In the following the will consider linear operator of $\mathbb{R}^N$ that acts on the vector $W(z)$ along with linear operator of $\mathbb{C}_D^N[z]$. Both of those operation can be represented using matrices, acting to the left (resp. to the right) of the coefficient matrix W for operator of $\mathbb{R}^N$ (resp. for operator of $\mathbb{C}_D^N[z]$).

2.3.3 Derivation and multiplication of polynomials

In the following, two particular operations on polynomials will be required to rewrite the equations of motion: taking the derivative of a vector of polynomials w.r.t a variable z_j, and multiplying a vector of polynomials by a given "scalar" polynomial. These operations are linear operations in the space of multivariate polynomials of degree D and can be represented as matrices that act onto the coefficients of the input vector of polynomials.

We consider first the derivative operation ∂_{z_j} for $1 \leq j \leq N$ applied to the (column) vector of polynomials $W(z)$. Following the results presented in Appendix B, it can be expressed as:

$$\partial_{z_j} W(z) = W \partial_{z_j} B(z) = W \nabla^j B(z) \tag{7}$$

where ∇^j is an $M \times M$ constant matrix of integers representing the operation ∂_{z_j} relative to the basis $B(z)$. Equation (7) simply states that the components of the derivative $\partial_{z_j} W(z)$ relative to the basis $B(z)$ are given by the matrix of coefficients $W\nabla^j$. The derivation operation ∂_{z_j} reduces the degree of the input polynomial by one, therefore the derivation matrices ∇^j are (block) lower triangular matrices (with blocks of zeros on the diagonal).

We now consider the multiplication of a (column) vector of polynomials $W(z)$ by a scalar polynomial $\lambda(z)$. Following the results presented in Appendix B, the product can be expressed as:

$$\lambda(z) W(z) = W \sum_m \lambda_m \Delta^m B(z) \tag{8}$$

where Δ^m is an $M \times M$ constant Boolean matrix representing the operation "multiply by $b_m(z)$" relative to the basis $B(z)$. The components of the product relative to $B(z)$ are given by the matrix of coefficients $W \sum_m \lambda_m \Delta^m$.

Note that some information about the monomials of degree greater than D is lost at this point because those monomials do not belong to the space $\mathbb{C}_D[z]$ and do not appear in the basis $B(z)$. This, however, is not a problem since we aim at computing a normal form up to degree D. If $m = 0$, we have $\Delta^0 = I_M$ (the identity matrix of size M). For $m \geq 1$, the multiplication operation "multiply fy $b_m(z)$" increases the degree of the input polynomial by $\deg(b_m(z))$. As a consequence, the multiplication matrices Δ^m are (block) upper triangular matrices (with blocs of zeros on the diagonal).

The sequence of matrices ∇^k for $1 \leq k \leq n$ and Δ^m for $0 \leq m \leq M-1$ are very convenient to represent the derivation and multiplication operations. They operate to the right of the matrix of coefficients of a given polynomial. They all are sparse matrices with a special block structure due to the grading of polynomials according to their total degree; they can be computed and stored prior to the normal form computation once the number of normal variables (n) and the degree of polynomial approximations (D) are known.

2.3.4 Homological equation

Substituting the change of variable $y = W(z)$ into the initial quadratic DAE (1), and recalling that the reduced dynamics is written as $\dot{z} = f(z)$, leads to the following *invariance equation* [21, 32]:

$$A\frac{\partial W}{\partial z}(z)f(z) = LW(z) + Q(W(z), W(z)) \tag{9}$$

We consider the polynomials $W(z) \in \mathbb{C}_D^N[z]$ and $f(z) \in \mathbb{C}_N^n[z]$ to be represented by their matrix of coefficients W ($N \times M$ matrix) and f ($n \times M$ matrix):

$$W(z) = W\ B(z) \text{ and } f(z) = f\ B(z) \tag{10}$$

Using the results of the previous section, the left-hand side of Equation (9) can be rewritten as:

$$A\frac{\partial W}{\partial z}(z)f(z) = A\sum_{j=1}^{n}\frac{\partial W}{\partial z_j}(z)f^j(z) = AW\sum_{m=0}^{M-1}\sum_{j=1}^{n} f_m^j \nabla^j \Delta^m B(z) = AW\Xi B(z) \tag{11}$$

This shows that the operation $\frac{\partial[\cdot]}{\partial z}f$ is represented by the matrix $\Xi = \sum_{m=0}^{M-1}\sum_{j=1}^{n} f_m^j \nabla^j \Delta^m$ relative to the basis B. The operator Ξ is a combination of the elementary operators $\nabla^j\Delta^m$ corresponding to the operation $b_m(z)\partial_{z_j}$ (i.e. derivation w.r.t. z_j followed by a multiplication by the monomial $b_m(z)$).

Let us now consider the right-hand side of Equation (9). Using the multiplication matrices defined in the previous section, it can be rewritten as:

$$LW(z) + Q(W(z), W(z)) = \left(LW + \sum_{m=0}^{M-1}\sum_{s=0}^{M-1} Q(W_m, W_s)b_m\Delta^s\right)B(z) \tag{12}$$

where b_m is the (row) vector associated to the monomial $b_m(z)$ (i.e. containing a 1 in position m and zeros elsewhere). Note that the product $b_m\Delta^s$ actually corresponds to extracting the m-th line of the matrix Δ^s, and that the product $Q(W_m, W_s)b_m\Delta^s$ will generates an $N \times M$ matrix of coefficients.

Gathering the previous results, the homological Equation (9) can be rewritten as an equality between vectors of polynomials as:

$$AW\sum_{m=0}^{M-1}\sum_{j=1}^{n} f_m^j \nabla^j \Delta^m B(z) = \left(LW + \sum_{m=0}^{M-1}\sum_{s=0}^{M-1} Q(W_m, W_s)b_m\Delta^s\right)B(z) \tag{13}$$

By equating each coefficient of the monomials $b_r(z)$ in $B(z)$, the previous expression can be re-written as an equality between $N \times M$ matrices of coefficients (each column $r+1$ corresponding to the coefficients of the monomial $b_r(z)$ for $r \in [0, M-1]$):

$$AW\sum_{m=0}^{M-1}\sum_{j=1}^{n} f_m^j \nabla^j \Delta^m = LW + \sum_{m=0}^{M-1}\sum_{s=0}^{M-1} Q(W_m, W_s)b_m\Delta^s \tag{14}$$

Doing so, the tedious task of balancing of the coefficients of a given monomial "by hand" is now replaced by equating columns of matrices between the left and right-hand side of Equation (14). The equation for a particular monomial $b_r(z)$ for $0 \leq r \leq M-1$ can be assembled simply by looking at the $r+1$-th column of the matrices in Equation (14).

2.4 Resolution procedure

We aim now at giving explicit expressions for the equations to be solved in order to find the coefficient matrices W and f. The special block structure of the operators ∇^j and Δ^m allow us to proceed sequentially by increasing degree.

2.4.1 Degree 0 (constant part)

We first consider the coefficient of the constant monomial $b_0(z) = 1$. The corresponding equation to be solved is obtained by equating the first column of Equation (14). The only terms appearing in the left-hand side are related to the constant part of the reduced dynamics and the only term appearing in the right-hand side are related to the constant part of the change of variable. The equation reads:

$$A\sum_{j=1}^{n} f_0^j W_j = LW_0 + Q(W_0, W_0) \tag{15}$$

Since the equilibrium point of the initial DAE system is the origin, an easy way to solve this equation, and avoid the coupling with higher degree coefficients $(W_j)_{1\leq j\leq n}$, is to take $f_0^j = 0$ for $1 \leq j \leq n$ and $W_0 = 0$.

At this point the constant terms can removed from the general homological Equation (14), which can be rewritten as :

$$AW\sum_{m=1}^{M-1}\sum_{j=1}^{n} f_m^j \nabla^j \Delta^m = LW + \sum_{m=1}^{M-1}\sum_{s=1}^{M-1} Q(W_m, W_s) b_m \Delta^s \tag{16}$$

2.4.2 Degree 1 (linear part)

Next, we consider the coefficients of the linear monomials $b_r(z) = z_r$, related to the $r+1$-th column of both sides of Equation (14), for $1 \leq r \leq n$. The only terms appearing in the left-hand side are related to the linear part of the reduced dynamics, and the only terms appearing in the right-hand side are related to the linear part of the change of coordinates. For a given $r \in \{1, n\}$, the equation for the coefficients of monomial $b_r(z)$ reads:

$$A\sum_{j=1}^{n} f_r^j W_j = LW_r \tag{17}$$

and can be rewritten as:

$$(Af_r^r - L)W_r + \sum_{j\neq r} f_r^j W_j = 0 \tag{18}$$

Recalling that we would like the reduced dynamics to be in its simplest form, we can choose $f_r^j = 0$ for $1 \leq j \neq r \leq n$ and we can choose any eigenmode to solve the remainder part of the equation e.g. $W_r = Y_r$ and $f_r^r = \lambda_r$. In the case of a reduced normal form, the number n of normal variables should be even, and one has to choose the complex conjugated pairs of eigenmodes associated to the physical modes of interest included in the reduced-order model.

This step actually corresponds to a linear change of variables that renders the reduced dynamics uncoupled. At this point, the reduced dynamics can be written as:

$$\dot{z}_r = \lambda_r z_r \tag{19}$$

for $1 \leq r \leq n$, and the change of variables reads:

$$y(z) = \sum_{r=1}^{n} Y_r z_r \tag{20}$$

where Y_r and λ_r are the chosen eigenshapes and eigenvalues.

2.4.3 Higher degree (nonlinear part)

We now turn to the resolution for higher degree monomials. We consider a given monomial $b_r(z)$ of degree $d \leq D$. Again, the equation to be solved can be assembled by looking at the $r+1$-th column of the homological equation. Based on the structure of the operator Ξ (see e.g. Equation (36) in the Duffing example in Section 3), we can clearly see that several terms are now participating in the left-hand side of the homological Equation (16):

- The "diagonal block" associated with (degree preserving) operators $z_m\partial_{z_j} = \nabla^j\Delta^m$ for $1 \leq j, m \leq n$. These terms are related to the degree d coefficients of the change of variable and the linear coefficients of the reduced dynamics (this is where the so-called resonance conditions appear)
- The first "upper diagonal block" associated with the operators $b_m(z)\partial_{z_j} = \nabla^j\Delta^m$ for all m such that $\deg(b_m) = d$. These terms are related to the degree d coefficient of the reduced dynamics and to the linear coefficient of the change of variables.
- The remainder "upper diagonal blocks" associated to the operators $b_m(z)\partial_{z_j} = \nabla^j\Delta^m$ for all m such that $1 < \deg(b_m) < d$. These terms are associated to the degree p ($1 < p < d$) coefficient of the reduced dynamics (and to the degree $d-p$ of the coefficients of the change of variables). These terms arise only due to the fact that the reduced dynamics cannot in general be put into linear form because of the resonance conditions. Note that these terms are known at this point of the resolution procedure and therefore are only participating in the right-hand side of the equation to be solved (along with the terms arising from the quadratic operator Q).

The equation for the coefficient of a general monomial $b_r(z)$ of degree d can be written as:

$$\underbrace{(\sum_{k=1}^{n}\alpha_{rk}\lambda_k)AW_r}_{\text{Diagonal block}} + \underbrace{\sum_{j=1}^{n} f_r^j AY_j}_{\text{First upper diag. block}} + \underbrace{\sum_{p} f_{m_p}^{j_p} AW_{k_p}}_{\text{remainder upper diag. blocks}} = LW_r + \sum_{j=1}^{n}\sum_{k=1}^{n}\epsilon_{jk}^r Q(W_j, W_k) \tag{21}$$

with $\sum_{k=1}^{n}\alpha_{rk} = d$ ($\alpha_{rk} \in \{0, 1, 2, \ldots, d\}$), and $\epsilon_{jk}^r = 1$ if $\deg[b_j(z)b_k(z)] = \deg[b_r(z)]$, $\epsilon_{jk}^r = 0$ otherwise.

In view of resolution, we rewrite the previous equation under the following form:

$$(\sigma_r A - L)\, W_r + \sum_{j=1}^{n} f_r^j AY_j = \sum_{j=1}^{n}\sum_{k=1}^{n}\epsilon_{jk}^r Q(W_j, W_k) - \sum_{p} f_{m_p}^{j_p} AW_{k_p} = R_r \tag{22}$$

with $\sigma_r = \sum_{k=1}^{n}\alpha_{rk}\lambda_k$. Note that the right-hand side is known at this point and will be denoted R_r. In the left-hand side we see appear the so-called resonance condition in the coefficient σ_r: if $\sigma_r = \lambda_s$, for a given s, then the operator $\sigma_r A - L$ in the left-hand side of Equation (22) becomes singular. The resolution proceeds as follows:

- if $\sigma_r A - L$ is not singular, then we can take $f_r^j = 0$ for $1 \leq j \leq n$ (we do not include any new terms in the reduced dynamics) and we obtain the coefficient for the change of variables as:

$$W_r = (\sigma_r A - L)^{-1} R_r \tag{23}$$

- if $\sigma_r = \lambda_s$, then the only terms we need to keep are the terms $f_r^{s_i} AY_{s_i}$ (where Y_{s_i} $i \in [1, R]$ are the possibly multiple eigenshapes associated to the eigenvalue λ_s, i.e. the resonant modes) to account for the component of the right-hand side parallel to the kernel of $\sigma_r A - L$ (i.e. parallel to the Y_{s_i}), and we can set all the other $f_r^j = 0$ for $1 \leq j \neq s_i \leq n$. To close the system, we impose that the vector of coefficients W_r is orthogonal to the kernel of $\sigma_r A - L$ generated by the left eigenvectors X_{s_i}, which generates an additional R equations. The system to be solved can be written as:

$$\begin{pmatrix} \sigma_r A - L & AY_{s_i, i\in[1,R]} & 0 \\ X_{s_i, i\in[1,R]}^T A & 0 & 0 \\ 0 & 0 & 1 \end{pmatrix} \begin{pmatrix} W_r \\ f_r^{s_i, i\in[1,R]} \\ f_r^{s_j, j\notin[1,R]} \end{pmatrix} = \begin{pmatrix} R_r \\ 0 \\ 0 \end{pmatrix} \tag{24}$$

At each degree $d \leq D$ there is M_d systems of equation to be solved corresponding to all the monomials $b_r(z)$ of degree d. The procedure is carried out sequentially by increasing degree until a reduced normal form of degree d is eventually computed.

2.5 Validity limit estimation for single mode reduction

We propose here a simple estimation of the validity limit when the reduced dynamics contains only two complex conjugate variables (single mode reduction). The normal variables z_1 and z_2 can be rewritten under polar form as $z_1 = \rho e^{i\theta}$ and $z_2 = \rho e^{-i\theta}$ with $\rho \in \mathbb{R}^+$ and $\theta \in \mathbb{R}$.

If we consider a particular component $W^j(z)$ of the change of variable (or of the reduced dynamics), it will be written under the form of a series in the variable ρ with coefficients depending (periodically) on the variables θ, and can be generally written as:

$$W^j(z) = W^j(\rho, \theta) = \sum_{d=0}^{D} a_d(\theta)\rho^d \tag{25}$$

If the series is computed to a high enough degree D, then the convergence radius of the series can be estimated using the traditional Cauchy or d'Alembert criterion [51], giving the maximum limit ρ_C (resp. ρ_A) for the (infinite) series to converge. The criteria are defined as:

$$\frac{1}{\rho_C} = \lim_{d\to+\infty} a_d^{1/d} \tag{26}$$

$$\frac{1}{\rho_A} = \lim_{d\to+\infty} \frac{a_{d+1}}{a_d} \tag{27}$$

Most of the time only even or only odd terms appear in the series and the d'Alembert criteria have to be adapted, e.g. for a series containing only even terms, the criterion becomes:

$$\frac{1}{\rho_A^2} = \lim_{l\to+\infty} \frac{a_{2l+2}}{a_{2l}} \tag{28}$$

The computation of the convergence radius for each variable can be realised for several values of the variables θ over $[0, 2\pi]$ to give a global estimation of the convergence of the results.

When the reduced dynamics contains more than two variables, other convergence criteria can be used, such as looking at the singularities of the homological operator as in [48]. One can also look at the singularities of the Jacobian of the reduced dynamics $J = \partial_z f$ to obtain information about the validity limit of the normal form expansion.

2.6 Comments

The method to compute the normal form is presented here starting from the general form of a quadratic DAE. This formalism has the advantage of being quite general and allows to push analytical development further. In addition, this formalism is also used in the Manlab package [52] and it is convenient to reuse the same input for the normal form computation.

We would like to point out, however, that the method can actually be applied to any polynomial DAE. Indeed, only the right-hand side of the homological equation will be affected, and the multiplication matrices can be used as many time as necessary to reach the degree of the polynomial nonlinearity. For example, if the quadratic operator Q is replaced with a cubic operator K, then the polynomial $K(W(z), W(z), W(z))$ can be written as:

$$K(W(z), W(z), W(z)) = \left(\sum_m \sum_s \sum_r K(W_m, W_s, W_r) b_m \Lambda^s \Lambda^r \right) B(z) \tag{29}$$

For a DAE that derives from a Hamiltonian, the inclusion of the reduced dynamics in the unknown is actually not necessary, and the reduced dynamics can be computed directly by imposing that the change of variable is canonical (i.e. preserve the symplectic form) at each degree. This should be considered in future work.

3 Illustration on a Duffing oscillator

To illustrate the proposed method we consider here a detailed application to a simple Duffing equation written as:

$$\ddot{u} + u + u^3 = 0 \tag{30}$$

We believe that the detailed application provides a good insight to the core aspects of the method and helps to show how it can easily be turned into an automated procedure for high degree normal form computation. The analytical expressions presented in this section are actually general and not limited to the Duffing oscillator; the results can be used to compute a single mode normal form (reduced dynamics with two variables only) of any quadratic DAE up to degree 3.

3.1 Definition of the quadratic system and eigenmodes

Defining the velocity $v = \dot{u}$ and the auxiliary variable $r = u^2$, the Duffing equation (30) is rewritten as the quadratic DAE (1) given in explicit form by:

$$\begin{pmatrix} 1 & 0 & 0 \\ 0 & 1 & 0 \\ 0 & 0 & 0 \end{pmatrix} \begin{pmatrix} \dot{u} \\ \dot{v} \\ \dot{r} \end{pmatrix} = \begin{pmatrix} 0 & 1 & 0 \\ -1 & 0 & 0 \\ 0 & 0 & 1 \end{pmatrix} \begin{pmatrix} u \\ v \\ r \end{pmatrix} + \begin{pmatrix} 0 \\ -ur \\ -u^2 \end{pmatrix} \tag{31}$$

The (right) linear eigenmodes (λ_k, Y_k) of the previous system are:

$$\lambda_1 = i, \lambda_2 = -i, \lambda_3 = \infty \tag{32}$$

associated to the following eigenvectors:

$$Y_1 = \begin{pmatrix} -i \\ 1 \\ 0 \end{pmatrix}, \; Y_2 = \begin{pmatrix} i \\ 1 \\ 0 \end{pmatrix}, Y_3 = \begin{pmatrix} 0 \\ 0 \\ 1 \end{pmatrix} \tag{33}$$

3.2 Detailed normal form computation up to degree 3

We consider here the computation of a normal form for the Duffing equation up to degree $D = 3$ in $n = 2$ variables $z = (z_1, z_2)$. The vector space $\mathbb{C}_D[z]$ is of dimension $M = 10$ and is generated by the basis:

$$B(z) = \left[1, \; z_1, \; z_2, \; z_1^2, \; z_1 z_2, \; z_2^2, \; z_1^3, \; z_1^2 z_2, \; z_1 z_2^2, \; z_2^3\right]^T \tag{34}$$

Once the basis B is known, the derivation and multiplication matrices can be computed easily by using the definition provided in Appendix B. For this application ($n = 2$, $D = 3$) the derivation and multiplication matrices are explicitly given in Appendix B. For each unknown polynomials there is $M = 10$ coefficients to be computed. The change of variable W (resp. the reduced dynamics f) of the Duffing oscillator will therefore consists in a 3×10 (resp. a 2×10) matrix of complex coefficients.

3.2.1 Constant and linear part

Following the procedure detailed in the previous section, the constant part of the change of variable and the reduced dynamics are set to zero: $W_0 = 0$, $f_0 = 0$ (first columns of W and f). The linear part of the change of variables consists in the two mode shapes $W_1 = Y_1$ and $W_2 = Y_2$, and the linear part of the reduced dynamics is taken as $f_1 = \begin{pmatrix} \lambda_1 \\ 0 \end{pmatrix} = \begin{pmatrix} i \\ 0 \end{pmatrix}$ and $f_2 = \begin{pmatrix} 0 \\ \lambda_2 \end{pmatrix} = \begin{pmatrix} 0 \\ -i \end{pmatrix}$.

3.2.2 nonlinear part

We first recall here the general homological Equation (16):

$$AW \sum_{m=1}^{M-1} \sum_{j=1}^{n} f_m^j \nabla^j \Delta^m = LW + \sum_{m=1}^{M-1} \sum_{s=1}^{M-1} Q(W_m, W_s) b_m \Delta^s \tag{35}$$

Taking into account that the constant and linear part of the normal form is known at this point, the operator $\Xi = \sum_{m=1}^{M-1} \sum_{j=1}^{n} f_m^j \nabla^j \Delta^m$ can be computed (see Appendix B) and expressed as:

$$\Xi = \left(\begin{array}{c|cc|ccc|ccc|c} 0 & 0 & 0 & 0 & 0 & 0 & 0 & 0 & 1 & 0 \\ \hline 0 & \lambda_1 & 0 & f_3^1 & f_4^1 & f_5^1 & f_6^1 & f_7^1 & f_8^1 & f_9^1 \\ 0 & 0 & \lambda_2 & f_3^2 & f_4^2 & f_5^2 & f_6^2 & f_7^2 & f_8^2 & f_9^2 \\ \hline 0 & 0 & 0 & 2\lambda_1 & 0 & 0 & 2f_3^1 & 2f_4^1 & 2f_5^1 & 0 \\ 0 & 0 & 0 & 0 & \lambda_1+\lambda_2 & 0 & f_3^2 & f_3^1+f_4^2 & f_5^2+f_4^1 & f_5^1 \\ 0 & 0 & 0 & 0 & 0 & 2\lambda_2 & 0 & 2f_3^2 & 2f_4^2 & 2f_5^2 \\ \hline 0 & 0 & 0 & 0 & 0 & 0 & 3\lambda_1 & 0 & 0 & 0 \\ 0 & 0 & 0 & 0 & 0 & 0 & 0 & 2\lambda_1+\lambda_2 & 0 & 0 \\ 0 & 0 & 0 & 0 & 0 & 0 & 0 & 0 & \lambda_1+2\lambda_2 & 0 \\ 0 & 0 & 0 & 0 & 0 & 0 & 0 & 0 & 0 & 3\lambda_2 \end{array}\right) \tag{36}$$

Degree 2 coefficients

The equations for the coefficients of the degree 2 monomials $b_r(z)$ for $3 \leq r \leq 5$ are given by looking at the columns 4 to 6 of the homological equation (i.e of the operator Ξ for the left-hand side of the equation, remembering that Ξ operates to the left of the coefficient matrix W). The three equations are given by:

- Coefficient of $b_3(z) = z_1^2$:

$$2\lambda_1 A W_3 + f_3^1 A Y_1 + f_3^2 A Y_2 = L W_3 + Q(Y_1, Y_1) \tag{37}$$

which can be rewritten as:

$$(2\lambda_1 A - L) W_3 + f_3^1 A Y_1 + f_3^2 A Y_2 = Q(Y_1, Y_1) \tag{38}$$

Since there is no resonance condition for this monomial, we can directly solve the equation by setting $f_3 = \begin{pmatrix} 0 \\ 0 \end{pmatrix}$ and $W_3 = (2iA - L)^{-1} Q(Y_1, Y_1)$.

- Coefficient of $b_4(z) = z_1 z_2$:

$$(\lambda_1 + \lambda_2) A W_4 + f_4^1 A Y_1 + f_4^2 A Y_2 = L W_4 + Q(W_1, W_2) + Q(W_2, W_1) \tag{39}$$

Again, there is no resonance condition and the resolution gives:
$f_4 = \begin{pmatrix} 0 \\ 0 \end{pmatrix}$ and $W_4 = -L^{-1} [Q(Y_1, Y_2) + Q(Y_2, Y_1)]$.

- Coefficient of $b_5(z) = z_2^2$:

$$2\lambda_2 A W_5 + f_5^1 A Y_1 + f_5^2 A Y_2 = L W_5 + Q(Y_2, Y_2) \tag{40}$$

which leads to $f_5 = \begin{pmatrix} 0 \\ 0 \end{pmatrix}$ and $W_5 = (-2iA - L)^{-1} Q(Y_2, Y_2)$.

In the case of the Duffing oscillator, the expressions for the coefficients of the change of variables are given by:

$$W_3 = \begin{pmatrix} 0 \\ 0 \\ -1 \end{pmatrix}, \; W_4 = \begin{pmatrix} 0 \\ 0 \\ 2 \end{pmatrix}, \; W_5 = \begin{pmatrix} 0 \\ 0 \\ -1 \end{pmatrix} \tag{41}$$

At this order only the change of variable is updated, mainly to take into account the constraints (only the last component the vectors of coefficients W_3 to W_5 is non zero). No additional terms are included in the reduced dynamics, which is still linear at this point.

Note that the column of the operator Ξ can be updated and simplified using the known coefficients f_r for $3 \leq r \leq 5$, leading to:

$$\Xi = \left(\begin{array}{c|cc|ccc|ccc|c} 0 & 0 & 0 & 0 & 0 & 0 & 0 & 0 & 1 & 0 \\ \hline 0 & \lambda_1 & 0 & 0 & 0 & 0 & f_6^1 & f_7^1 & f_8^1 & f_9^1 \\ 0 & 0 & \lambda_2 & 0 & 0 & 0 & f_6^2 & f_7^2 & f_8^2 & f_9^2 \\ \hline 0 & 0 & 0 & 2\lambda_1 & 0 & 0 & 0 & 0 & 0 & 0 \\ 0 & 0 & 0 & 0 & \lambda_1 + \lambda_2 & 0 & 0 & 0 & 0 & 0 \\ 0 & 0 & 0 & 0 & 0 & 2\lambda_2 & 0 & 0 & 0 & 0 \\ \hline 0 & 0 & 0 & 0 & 0 & 0 & 3\lambda_1 & 0 & 0 & 0 \\ 0 & 0 & 0 & 0 & 0 & 0 & 0 & 2\lambda_1 + \lambda_2 & 0 & 0 \\ 0 & 0 & 0 & 0 & 0 & 0 & 0 & 0 & \lambda_1 + 2\lambda_2 & 0 \\ 0 & 0 & 0 & 0 & 0 & 0 & 0 & 0 & 0 & 3\lambda_2 \end{array}\right) \tag{42}$$

Degree 3 coefficients

The equations for the coefficients of the degree 3 monomials $b_r(z)$ for $6 \leq r \leq 9$ are given by looking at columns 5 to 10 of the homological equation. Out of the four equations, two are related to (natural) resonance conditions associated with the relations $2\lambda_1 + \lambda_2 = \lambda_1$ and $\lambda_1 + 2\lambda_2 = \lambda_2$ (see the diagonal of operator Ξ). The four equations are given by:

- Coefficient of $b_6(z) = z_1^3$ (non-resonant):

$$3\lambda_1 A W_6 + f_6^1 A Y_1 + f_6^2 A Y_2 = L W_6 + Q(Y_1, W_3) + Q(W_3, Y_1) \tag{43}$$

whic can be rewritten as:

$$(3\lambda_1 A - L) W_6 + f_6^1 A Y_1 + f_6^2 A Y_2 = Q(Y_1, W_3) + Q(W_3, Y_1) \tag{44}$$

Since there is no resonance condition for this monomial, we can directly solve the equation by setting $f_6 = \begin{pmatrix} 0 \\ 0 \end{pmatrix}$ and $W_6 = (3iA - L)^{-1} [Q(Y_1, W_3) + Q(W_3, Y_1)]$.

- Coefficient of $b_7(z) = z_1^2 z_2$ (resonant):

$$(2\lambda_1 + \lambda_2) A W_7 + f_7^1 A Y_1 + f_7^2 A Y_2 = L W_7 + Q(Y_1, W_4) + Q(W_4, Y_1) + Q(Y_2, W_3) + Q(W_3, Y_2) \tag{45}$$

which can be rewritten as:

$$(\lambda_1 A - L)W_7 + f_7^1 AY_1 + f_7^2 AY_2 = Q_7 \tag{46}$$

Since $(\lambda_1 A - L)$ is singular, we have to keep the term $f_7^1 AY_1$ to solve the equation. The system to be solved is given as:

$$\begin{pmatrix} \lambda_1 A - L & AY_1 & 0 \\ X_1^T A & 0 & 0 \\ 0 & 0 & 1 \end{pmatrix} \begin{pmatrix} W_7 \\ f_7^1 \\ f_7^2 \end{pmatrix} = \begin{pmatrix} Q_7 \\ 0 \\ 0 \end{pmatrix} \tag{47}$$

- Coefficient of $b_8(z) = z_1 z_2^2$ (resonant): as for the precedent term, the equation is rewritten as:

$$(\lambda_2 A - L)W_8 + f_8^1 AY_1 + f_8^2 AY_2 = Q_8 \tag{48}$$

Since $(\lambda_2 A - L)$ is singular, we have to keep the term $f_8^2 AY_2$ to solve the equation. The system to be solved is given as:

$$\begin{pmatrix} \lambda_2 A - L & AY_2 & 0 \\ X_2^T A & 0 & 0 \\ 0 & 0 & 1 \end{pmatrix} \begin{pmatrix} W_8 \\ f_8^2 \\ f_8^1 \end{pmatrix} = \begin{pmatrix} Q_7 \\ 0 \\ 0 \end{pmatrix} \tag{49}$$

- Coefficient of $b_9(z) = z_2^3$ (non resonant): as for the first term, the equation is rewritten equation as:

$$(3\lambda_2 A - L)W_9 + f_8^1 AY_1 + f_8^2 AY_2 = Q_9 \tag{50}$$

The resolution gives $f_9 = \begin{pmatrix} 0 \\ 0 \end{pmatrix}$ and $W_9 = (-3iA - L)^{-1} Q_9$.

The numerical results for the Duffing oscillator can be summarized as:

$$W_6 = \frac{1}{8}\begin{pmatrix} i \\ -3 \\ 0 \end{pmatrix},\ W_7 = \frac{3}{4}\begin{pmatrix} i \\ 1 \\ 0 \end{pmatrix},\ W_8 = \frac{3}{4}\begin{pmatrix} -i \\ 1 \\ 0 \end{pmatrix},\ W_9 = -\frac{1}{8}\begin{pmatrix} i \\ 3 \\ 0 \end{pmatrix} \tag{51}$$

and

$$f_6 = \begin{pmatrix} 0 \\ 0 \end{pmatrix},\ f_7 = \frac{3}{2}\begin{pmatrix} i \\ 0 \end{pmatrix},\ f_8 = -\frac{3}{2}\begin{pmatrix} 0 \\ -i \end{pmatrix},\ f_9 = \begin{pmatrix} 0 \\ 0 \end{pmatrix} \tag{52}$$

At degree 3, two terms are added to the reduced dynamics to take into account the resonant terms appearing naturally in the homological equation. The change of variable is also updated in order to take into account the curvature of the invariant manifold.

3.2.3 Sum up normal form Duffing order 3

For the normal form of the Duffing equation (written as a quadratic DAE) up to order 3, the change of variables is given by:

$$y = \begin{pmatrix} u \\ v \\ r \end{pmatrix} = W(z) = WB(z) = \left(\begin{array}{c|cc|ccc|cccc} 0 & -i & i & 0 & 0 & 0 & \frac{i}{8} & \frac{3i}{4} & -\frac{3i}{4} & -\frac{i}{8} \\ 0 & 1 & 1 & 0 & 0 & 0 & -\frac{3}{8} & \frac{3}{4} & \frac{3}{4} & -\frac{3}{8} \\ 0 & 0 & 0 & -1 & 2 & -1 & 0 & 0 & 0 & 0 \end{array}\right) \begin{pmatrix} 1 \\ z_1 \\ z_2 \\ z_1^2 \\ z_1 z_2 \\ z_2^2 \\ z_1^3 \\ z_1^2 z_2 \\ z_1 z_2^2 \\ z_2^3 \end{pmatrix} \tag{53}$$

and the reduced dynamics by:

$$\dot{z} = f(z) = fB(z) = \left(\begin{array}{c|cc|ccc|cccc} 0 & i & 0 & 0 & 0 & 0 & 0 & \frac{3i}{2} & 0 & 0 \\ 0 & 0 & -i & 0 & 0 & 0 & 0 & 0 & -\frac{3i}{2} & 0 \end{array}\right) \begin{pmatrix} 1 \\ z_1 \\ z_2 \\ z_1^2 \\ z_1 z_2 \\ z_2^2 \\ z_1^3 \\ z_1^2 z_2 \\ z_1 z_2^2 \\ z_2^3 \end{pmatrix} \tag{54}$$

which is simply rewritten as:

$$\begin{pmatrix}\dot{z}_1\\ \dot{z}_2\end{pmatrix} = \begin{pmatrix} iz_1 + \frac{3i}{2}z_1^2 z_2 \\ -iz_2 - \frac{3i}{2}z_1 z_2^2 \end{pmatrix} \tag{55}$$

If we set $z_1 = \rho e^{i\theta}$ and $z_2 = \rho e^{-i\theta}$, then the change of variable is rewritten as:

$$W(\rho,\theta) = \begin{pmatrix}u\\ v\\ r\end{pmatrix} = \begin{pmatrix} 2\rho\sin\theta + \rho^3\sin\theta(\sin^2\theta - \frac{9}{4}) \\ 2\rho\cos\theta + \rho^3\cos\theta(-3\cos^2\theta + \frac{15}{4}) \\ 4\rho^2\sin^2\theta \end{pmatrix} \tag{56}$$

and the reduced dynamics can be rewritten as:

$$\dot{\rho} = 0 + o(\rho^3)$$
$$\dot{\theta} = \omega = 1 + \frac{3}{2}\rho^2 + o(\rho^3)$$

The first equation in the reduced dynamics is related to the conservation of energy in the system, and the second equation says that the angular frequency only depends on the amplitude ρ, and is therefore a constant (since ρ is constant). It directly gives the expression for the backbone curve of the Duffing oscillator parametrised by the parameter ρ: $(\omega(\rho), u_{max}(\rho))$.

3.3 Normal form at higher degree and convergence results

In this section we aim at assessing the validity of the normal form results and give some information about the convergence of the series. A reference solution can be computed analytically for the free Duffing oscillator using Jacobi elliptic functions. The evolution of the natural frequency as a function of the initial amplitude u_0 (zero initial velocity) is given by the following (see [53]):

$$\omega_{\text{exact}} = \frac{\pi\sqrt{1+u_0^2}}{2K(m)} \tag{57}$$

where K is the elliptic integral of modulus $m = \sqrt{\frac{u_0^2}{2(1+u_0^2)}}$. This reference solution will be used to compare the backbone curves and compute the error. In addition to the exact solution, we also consider a single harmonic approximation $u(t) = u_0\cos\omega t$ (Harmonic Balance Method, HBM) for comparison purposes; in that case the approximated angular frequency for the Duffing oscillator is given by:

$$\omega_{\text{hbm}} = \sqrt{1 + \frac{3}{4}u_0^2} \tag{58}$$

The normal form for the Duffing oscillator is computed using the proposed method for degree 3 up to 31 and the results are compared to the reference solution in Figure 1. The backbone curves are compared on the left part of the figure and one can observe a very good agreement between the normal form and the reference results for low to moderate amplitudes. The normal form precision is obviously increased for higher degree. The relative error to the exact solution is depicted on the right part of Figure 1 and one can see that increasing the degree of the normal form reduces considerably the error.

Even if the HBM solution (with a single harmonic) seems to have a better global behaviour from the backbone point of view, it can be seen in the error graph that a normal form with high enough degree is actually orders of magnitude more precise (in its convergence domain).

To study the limit of validity of the results, we use the normal form at degree 31 to compute an estimation of the convergence radius of the various series (reduced dynamics and change of coordinates) using the d'Alembert and Cauchy criteria presented in Section 2.5. The estimated convergence radius is plotted against the normal form degree in Figure 2. One can see that both the d'Alembert and Cauchy criteria seem to converge and that they give very similar convergence radius estimation. This indicates that the normal form series are indeed convergent in their validity domain. Note that the convergence of the Cauchy coefficients seems to be slower than the d'Alembert's one, but both criteria lead to roughly the same estimated convergence radius. In this case, it is the series associated with the auxiliary variables that leads to the smallest convergence radius (using the d'Alembert criteria). This allows for an estimation of the convergence radius ρ^* of the series, and hence an upper validity bound on the amplitude u (see Figure 1. This means that even if we increase the degree of the normal form, the quality of the results will not be improved for amplitudes above the validity bound.

Since the coefficients of the series depend on the variable θ (recall $z_1 = \rho e^{i\theta}$ and $z_2 = \rho e^{-i\theta}$), which can be seen as a parameter describing the time along the period of the solution, the radius of convergence also depends on θ, and its evolution is depicted in Figure 3 for the d'Alembert and the Cauchy criterion. The estimated radius of convergence is taken as the minimum over θ of the convergence radius of all series (change of variables and reduced dynamics) using the d'Alembert criteria.

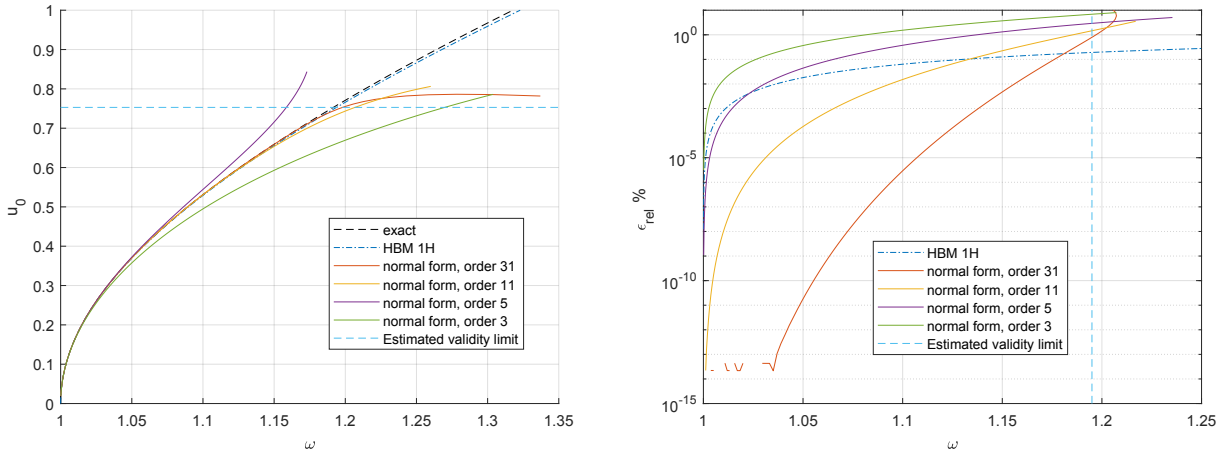

Figure 1: Comparison between exact solution and normal form (degree 3 to 31) for the Duffing oscillator. Left plot: evolution of the fundamental angular frequency ω as a function of the initial amplitude u_0. Right plot: relative error (in %) on the angular frequency between the exact and normal form solution. Single harmonic HBM results are also included for comparison purposes

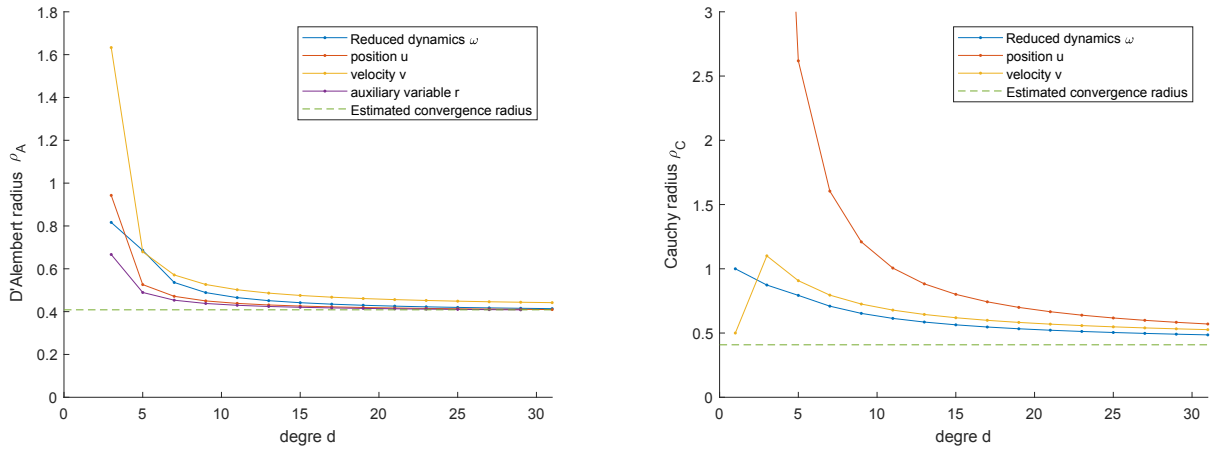

Figure 2: Left plot: Evolution of the d'Alemberts coefficients as a function of the degree d (for $\theta = 0$). Right plot: Evolution of the Cauchy coefficients as a function of the degree d (for $\theta = 0$).

4 Application to the Simple Pendulum system

In this section, we present the application of the normal form computation to the case of a free (unforced) simple pendulum, composed of a unit mass $m = 1$ attached to a massless rod of unit length $l = 1$ inside a constant vertical acceleration field $g = 1$.

With this example, we would like to show that the results of the normal form depend on the parametrisation used to recast the original dynamics under a quadratic ODE. Having in mind the application of the normal form to a geometrically exact beam finite-elements model where quaternions are used for parametrisation of rotations, we will first present the simple pendulum system using several types of motion parametrisation, resulting in different kinds of quadratic DAE able to represent the same mechanical system. A comparison is then drawn between the different models relative to the accuracy and the validity range of the normal form results.

4.1 Presentation of the parametrisation

The easiest way to represent the motion of the pendulum is to consider the angle θ between the rod and the vertical direction. In this case, the kinetic (T) and potential (U) energy are given by:

$$T = \frac{1}{2}\dot{\theta}^2, \; U = -\cos\theta \tag{59}$$

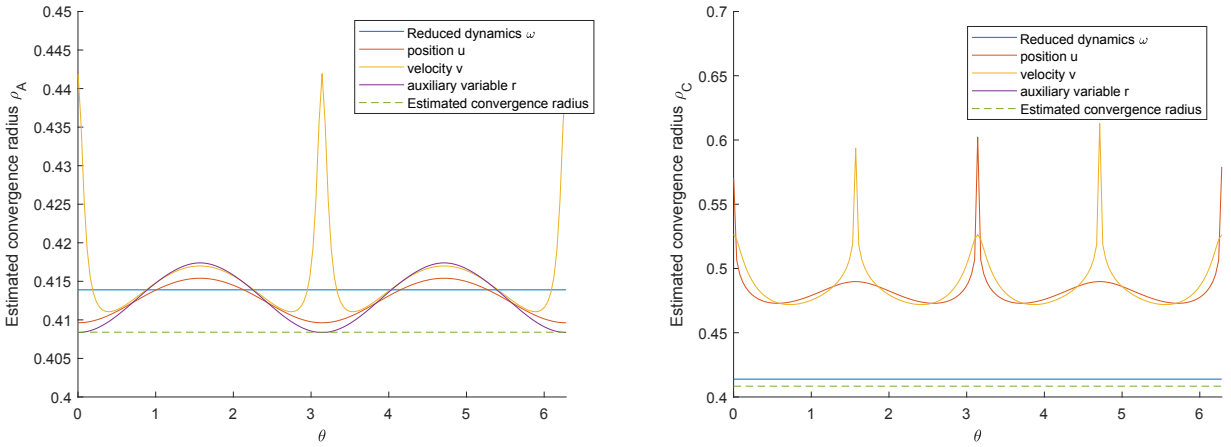

Figure 3: Evolution of the estimated convergence radius ρ_A and ρ_C as a function of the angle θ (position along the period) for the different series of the reduced dynamics ($\omega = \dot{\theta}$) and the change of variables (u, v, r). Left: d'Alembert coefficients, Right: Cauchy coefficients

and the equation of motion can be written as:

$$\ddot{\theta} + \sin\theta = 0 \tag{60}$$

Several parametrisation are proposed here for the simple pendulum based on the approach used to recast the original system under a quadratic DAE. They can be sorted into three categories:

- A direct Taylor expansion of the sine terms at various order, followed by the definition of the needed auxiliary variables to have a quadratic system. These systems will be termed "Taylor X" where X is the degree of the Taylor expansion of the sine.
- A Lagrangian approach base on the family of parametrisation $p_0 = \cos(\theta/n)$, $p_3 = \sin(\theta/n)$ for a given $n \in \mathbb{N}$, subject to the constraint $p_0^2 + p_3^2 = 1$. For $n = 1$, one recovers the Cartesian parametrisation, $n = 2$ correspond to the quaternion-like parametrisation, and $n \geq 3$ gives rise to a series of other parametrisations. Those systems will be termed "Chebichev n".
- A mixed approach where we directly substitute the parameters (p_0, p_3) in the equation of motion, and use an ODE to define the sine function. These systems will be termed "ODE Sine n".

Details about each kind of parametrisation is given in the following.

4.1.1 Taylor X

To transform the equation of motion into a quadratic DAE, one can use a Taylor expansion of the sine function around the equilibrium point (up to a reasonable order) so that the nonlinearity becomes polynomial so that the system can then be recast under a quadratic DAE easily. To exemplify this procedure, we consider a Taylor expansion at order 5 for the sine function. In this case, the equation of motion is approximated by the following:

$$\ddot{\theta} + \theta - \frac{\theta^3}{6} + \frac{\theta^5}{120} = 0 \tag{61}$$

Introducing two auxiliary variables $a = \theta^2$ and $b = a^2$, the equation of motion can be rewritten under the form of a quadratic DAE as follows:

$$\dot{\theta} = \omega \tag{62}$$

$$\dot{\omega} = -\theta + \frac{a\theta}{6} - \frac{b\theta}{120} \tag{63}$$

$$0 = a - \theta^2 \tag{64}$$

$$0 = b - a^2 \tag{65}$$

The resulting quadratic DAE is centred around the origin and the proposed procedure to compute the normal form can be applied directly.

4.1.2 Chebichev n

In the following, we use a (family of) two dof parametrisation for the motion of the pendulum, resulting in a (family of) polynomial DAE that can then be recast under quadratic form. We consider an integer $n \in \mathbb{N}^*$ and we define the two following variables:

$$p_0 = \cos\frac{\theta}{n} \tag{66}$$

$$p_3 = \sin\frac{\theta}{n} \tag{67}$$

Considering the n-th Chebichev polynomial (of the first kind) T_n, defined such that $\cos nx = T_n(\cos x)$, and setting $nx = \theta$, one can write the potential energy of the pendulum as:

$$U = -\cos\theta = -T_n(\cos\frac{\theta}{n}) = -T_n(p_0) \tag{68}$$

Considering the time derivatives of Equation (66), we can write the kinetic energy as:

$$T = \frac{n^2}{2}(\dot{p}_0^2 + \dot{p}_3^2) \tag{69}$$

Finally we introduce the constraint linking p_0 and p_3 as:

$$p_0^2 + p_3^2 - 1 = 0 \tag{70}$$

Using a Lagrange multiplier λ to take into account the constraint, and Euler- Lagrange equation to derive the equation of motion, one obtains the following (family of) equations for the simple pendulum:

$$n^2\ddot{p}_0 - \frac{\partial T_n}{\partial p_0} = 2\lambda p_0 \tag{71}$$

$$n^2\ddot{p}_3 = 2\lambda p_3 \tag{72}$$

$$p_0^2 + p_3^2 - 1 = 0 \tag{73}$$

Since T_n is a polynomial, the previous equation is a DAE with polynomial nonlinearities and can be recast to a quadratic form with no complications.

The idea of using such parametrisations is that if one chooses a large value for n, then variables p_0 and p_3 have a lower range of variation and can be very well captured by low order approximation in the normal form computation. However, as n increases, the degree of the equation of motion increases as well and more and more auxiliary variables are needed for the quadratic recast. Some examples for particular values of n are given in Appendix C.

4.1.3 ODE for $\sin\theta/n$

Another way to represent the pendulum motion under a quadratic DAE is to consider the rotation speed $\omega = \dot{\theta}$ and to introduce two more unknowns as $c = \cos\theta$ and $s = \sin\theta$. The sine function can be defined by the differential equation $\dot{s} = \Omega c$ along with the constraint $c^2 + s^2 - 1 = 0$. In this case the pendulum equation can be rewritten as:

$$\dot{\omega} = -s \tag{74}$$

$$\dot{s} = \omega c \tag{75}$$

$$0 = c^2 + s^2 - 1 \tag{76}$$

$$\tag{77}$$

which is in the form of a quadratic DAE (with non-zero equilibrium).

An alternative way to define the pendulum equation in this framework is to consider a quaternion-like parametrisation. In this case the additional unknowns are defined as $p_0 = \cos\frac{\theta}{2}$ and $p_3 = \sin\frac{\theta}{2}$, linked through the differential equation $\dot{p}_3 = \frac{1}{2}\dot{\theta}p_0$ and the constraint $p_0^2 + p_3^2 - 1 = 0$. In this case, one has $\sin\theta = 2\sin\frac{\theta}{2}\cos\frac{\theta}{2} = 2p_0p_3$ and the pendulum equation can be rewritten as:

$$\dot{\omega} = -2p_0p_3 \tag{78}$$

$$\dot{p}_3 = \frac{1}{2}\omega p_0 \tag{79}$$

$$0 = p_0^2 + p_3^2 - 1 \tag{80}$$

$$\tag{81}$$

4.2 Details on the normal form computation

We consider here the computation of a normal form for the simple pendulum system by applying the proposed method to the various quadratic DAE representing the equation of motion. For all systems, the input to the computation is defined in the same way and the operators A and L are provided as constant (sparse) matrices, and the quadratic operator Q can be provided directly using a function/routine.

The system is first set around the origin if the equilibrium is not zero. Then, the complex eigenmodes of the system are computed using the operators A and L. In the case of the pendulum, only the two modes associated to the oscillatory solution (i.e to the purely complex (conjugated) eigenvalues) are kept as an input for the computation, leading to a normal form containing only two (complex conjugated) normal variables z_1 and z_2.

4.3 Solution computation and comparison

In the following, we consider only the free motion of the pendulum when subjected to an initial displacement (zero initial velocity). We consider periodic solutions and aim to compute the evolution of the oscillation's period as a function of the initial amplitude (nonlinear mode / backbone curves) using the normal form for the several types of quadratic DAE presented in the previous section.

4.3.1 Reference solution

The reference solution for the pendulum's oscillation period can be derived analytically by first transforming the pendulum equation into a Duffing oscillator and then using Jacobi Elliptic integrals (see e.g. [53]). If we define θ_0 as the initial amplitude of the pendulum, then the oscillation period $T = T(\theta_0)$ can be expressed as:

$$T(\theta_0) = 4K(m) = 4\int_0^1 \sqrt{(1-t^2)(1-mt^2)}\, dt \tag{82}$$

where K is the complete elliptic integral of the first kind and $m = \sin^2 \frac{\theta_0}{2}$ is the modulus. The angular pulsation of the oscillation is given by $\omega(\theta_0) = \frac{2\pi}{T(\theta_0)}$. This expression will constitute the reference solution for all comparisons.

4.3.2 "Taylor X" results

We first consider here the case where the pendulum is parametrised using a single dof θ, and where the sine function appearing in the equation of motion is expanded using Taylor expansion. For comparison purposes we consider Taylor expansions at order $X = 11$ and $X = 21$. After a quadratic recast, the normal form is computed up to degree $d = 3, 5, 7, 21, 45$ for each system.

Figure 4 represents the evolution of the angular frequency of the pendulum oscillation as a function of $\sin\theta_0$. It can be observed that the results are independent of the degree of the Taylor expansion. It can be observed that increasing the degree of the normal form increase the quality of the results, and that the backbone barely depends on the Taylor expansion order X (which means that $X = 11$ is a good enough approximation in this case). The difference can only been seen for a normal form at order 45 where the error for a Taylor expansion at order $X = 21$ is smaller that the one for $X = 11$.

4.3.3 "Chebichev n" results

We consider here the case of the Chebichev n parametrisation for $n = 1, 2, 4$ (see Appendix C). After a quadratic recast, the normal form is computed up to degree $d = 3, 5, 7, 21, 45$ for each system.

Figure 6 represents the evolution of the angular frequency of the pendulum oscillation as a function of $\sin\frac{\theta_0}{2}$. It can be observed that for a given normal form degree D, the results are better as the parameter n increases. A possible explanation is the fact that the variable $p_3 = \sin\theta/n$ will have smaller and smaller amplitude as n increases, and is therefore easier to develop into a series. Again, for a given n, it can be observed that increasing the degree of the normal form increases the quality of the results. The results are in good agreement with the reference solution and the best results are given for the normal form at degree 45 using the the parametrisation with $n = 4$.

4.3.4 "ODE sine n" results

We consider here the case of the "ODE sine n" parametrisation for $n = 1, 2$. After a quadratic recast, the normal form is computed up to degree $d = 3, 5, 7, 21, 45$ for each system.

Figure 8 represent the evolution of the angular frequency of the pendulum oscillation as a function of $\sin\theta_0$. As in the previous case, it can be observed that for a given normal form degree D, the result are better as the parameter n increases. Again, the results are in good agreement with the reference solution and the best results are obtained for the parametrisation $n = 2$ at degree $D = 45$.

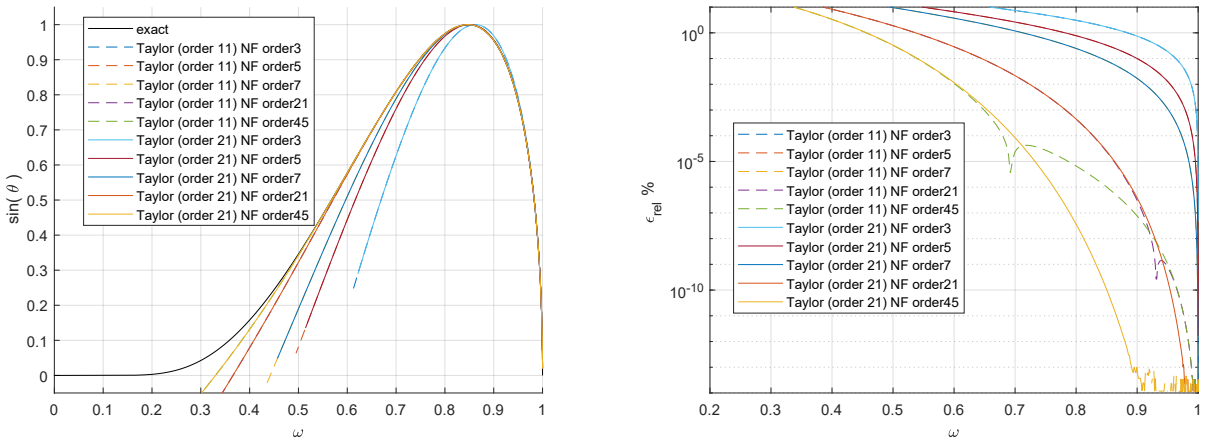

Figure 4: Comparison between exact solution and normal form (degree 3 to 45) for Taylor expansion (order 11 and 21). Left plot: evolution of the fundamental angular frequency ω as a function of the (sine) of the initial angle amplitude θ. Right plot: relative error (in %) on the angular frequency between the exact and normal form solution

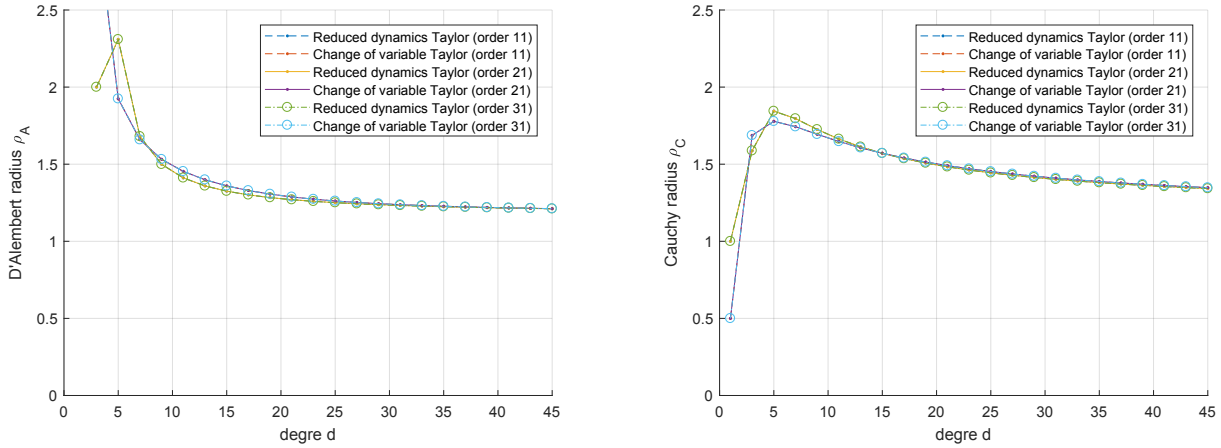

Figure 5: Left plot: Evolution of the d'Alemberts radius of convergence ρ_A a function of the degree d (for $\theta = 0$). Left plot: Evolution of the Cauchy radius of convergence ρ_C as a function of the degree d (for $\theta = 0$).

4.4 Comparison between the various parametrisation

Finally, we compare the different formulations by considering the normal form at degree $D = 45$ of each considered parametrisation for the simple pendulum. The results are presented in Figure 10. One can see that the worst parametrisation is the Cartesian parametrisation (Chebichev 1) as it gives the highest error. The ODE sine formulation for $n = 1, 2$ and the Chebichev 2 and 3 have a similar intermediary error level. The Taylor X formulation seems to give the best results as it gives the lowest error on the largest angular frequency range. One can conclude that in this case, a Taylor expansion at order 11 is barely sufficient to compute a normal form for the simple pendulum. Note however that a quaternion-like formulation (Chebichev 2) yields a reasonable error level over a relatively large angular frequency range.

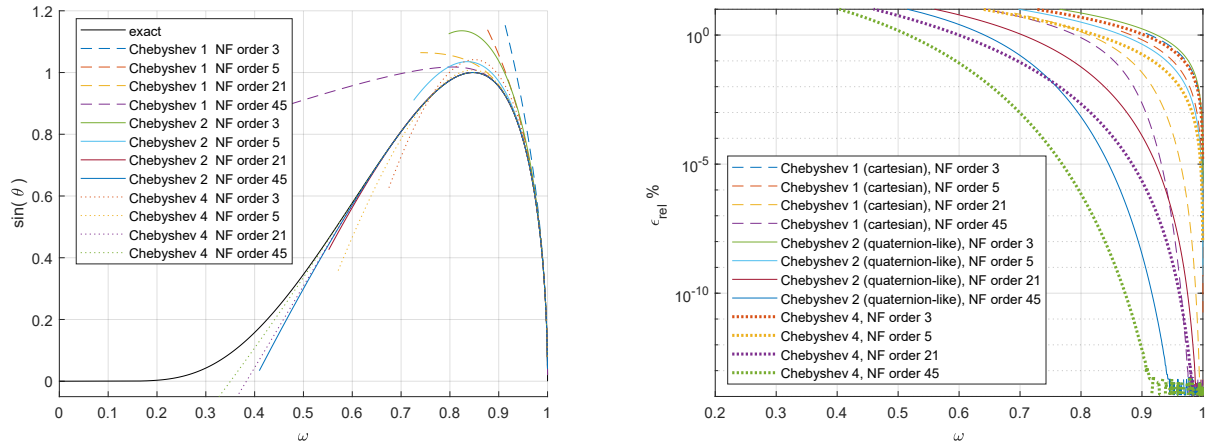

Figure 6: Comparison between exact solution and normal form (degree 3 to 45) when using the Chebichev parametrisation (see Appendix C) for $n = 1, 2$ and 4. Left plot: evolution of the fundamental angular frequency ω as a function of the (sine) of the initial angle amplitude θ. Right plot: relative error (in %) on the angular frequency between the exact and normal form solution

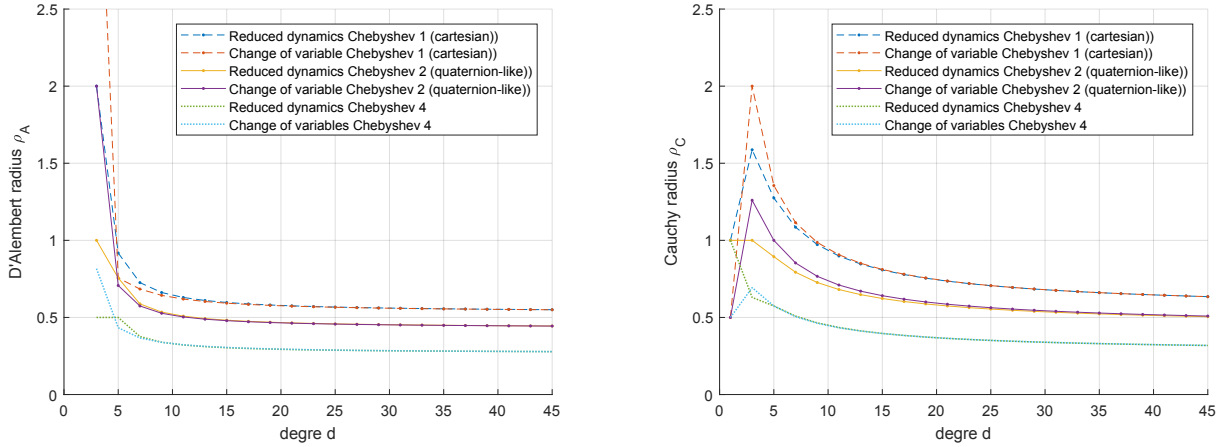

Figure 7: Left plot: Evolution of the d'Alembert radius of convergence ρ_A a function of the degree d (for $\theta = 0$). Left plot: Evolution of the Cauchy radius of convergence ρ_C as a function of the degree d (for $\theta = 0$).

5 Clamped-Clamped beam with Von Kármán model

In this section, we consider a clamped-clamped beam with geometric nonlinearities modelled using Von Kármán hypothesis. This allows us to consider a model of intermediate complexity before turning to the case of a full FE model as a last application.

5.1 Description of the system

We consider a clamped-clamped straight beam of length L with a homogeneous cross section of thickness h, area S and second moment of area I, made out of a homogeneous and isotropic material. The nonlinearities in this case are due to the coupling between the axial strain and the transverse displacement, and can be well-captured by a von Kármán model with neglected axial inertia [54, 55]. In this case, the continuous partial differential equations for the transverse displacement can be expressed under normalised form as:

$$\begin{aligned} \ddot{v} + v'''' - \alpha T v'' &= 0 \\ T &= \tfrac{1}{2}\int_0^1 (v')^2 dx \end{aligned} \tag{83}$$

where $v(x,t)$ is the transverse displacement field normalised by the thickness h (i.e. $v(x,t) = v^*(x,t)/h$ with $v^*(x,t)$ the dimensioned displacement), $x \in [0,1]$ is the normalised location along the middle axis of the beam (i.e. $x = x^*/L$ with x^* the dimensioned location), t is the normalised time, $\circ' = \partial \circ /\partial x$, $\dot{\circ} = \partial \circ /\partial x$, $T(t)$ is the (normalised) axial tension in the beam and $\alpha = Sh^2/I$ is a dimensionless parameter that depends on the cross section geometry only. In this text, a rectangular cross section is considered such that $\alpha = 12$ [55].

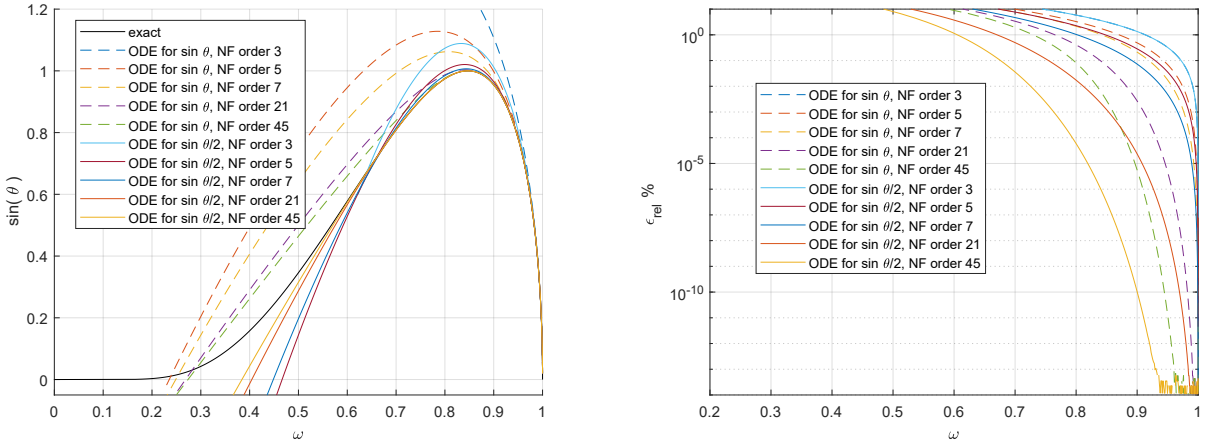

Figure 8: Comparison between exact solution and normal form (degree 3 to 45) when using an ODE to define $\sin\theta$ (see Equation (74)) or $\sin\theta/2$ (Equation (78)). Right plot: evolution of the fundamental angular frequency ω as a function of the (sine) of the initial angle amplitude θ. Right plot: relative error (in %) on the angular frequency between the exact and normal form solution

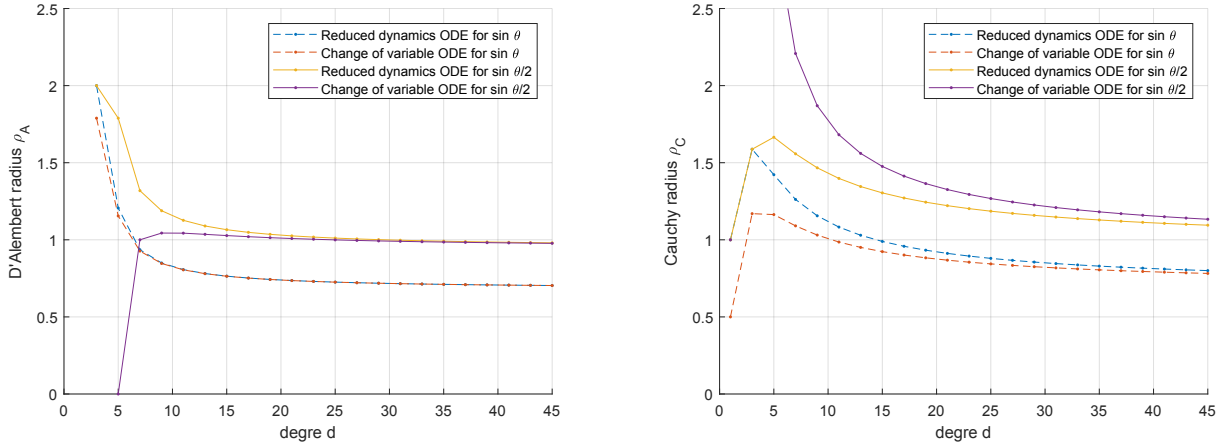

Figure 9: Left plot: Evolution of the d'Alemberts radius of convergence ρ_A a function of the degree d (for $\theta = 0$). Right plot: Evolution of the Cauchy radius of convergence ρ_C as a function of the degree d (for $\theta = 0$).

The continuous model is first discretised using the first transverse linear mode shapes Φ_j of the clamped clamped beam, in order to express the displacement v as:

$$v(x,t) = \sum_{j=1}^{N_{\text{mode}}} q_j(t)\Phi_j(x) \tag{84}$$

where $q_j(t)$ is the modal coordinate of the j-th transverse linear mode and N_{mode} is the number of retained modes in the expansion. Expanding the continuous equation of motion onto the reduced mode shape basis leads to the following set of second order differential equation for the variables $\{q_j\}_{1\leq j\leq N_{\text{mode}}}$:

$$\ddot{q}_j + \omega_j^2 q_j + \frac{1}{2}\alpha \sum_{k,l,m=1}^{N_{\text{mode}}} \Gamma_{jk}\Gamma_{lm}\ q_k q_l q_m = 0 \tag{85}$$

where ω_j are the natural angular frequencies of the transverse modes, defined as:

$$\omega_j = k_j^2, \tag{86}$$

with $\cosh k_j \cos k_j = 1$ and Γ_{jk} are constant coefficients defined as:

$$\Gamma_{jk} = \int_0^1 \phi_j'(x)\phi_k'(x)\,\mathrm{d}x, \tag{87}$$

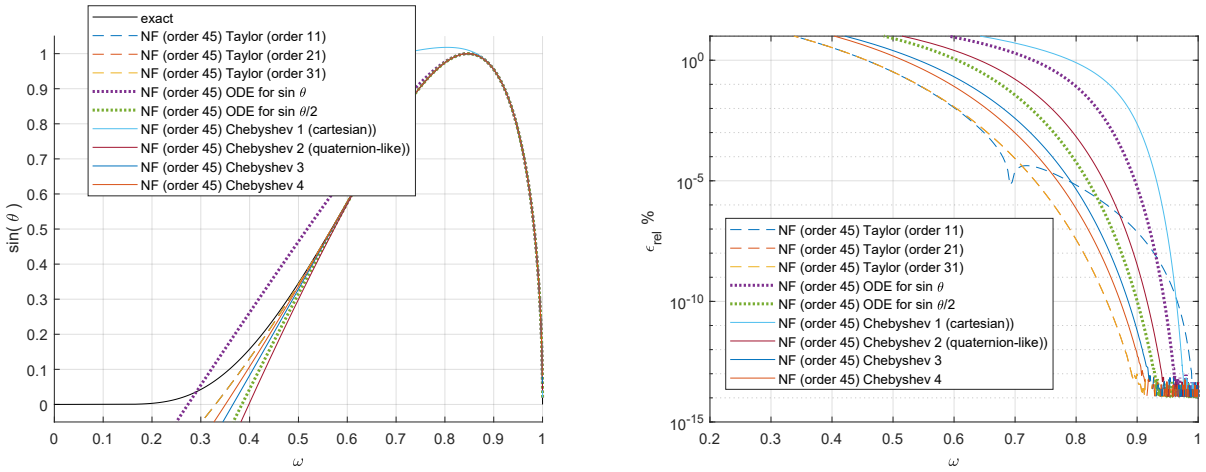

Figure 10: Comparison between exact solution and normal form (at degree 45) for the different formulation for the pendulum equation of motion. Left plot: evolution of the fundamental angular frequency ω as a function of the (sine) of the initial angle amplitude θ. Right plot: relative error (in %) on the angular frequency between the exact and normal form solution

if the mode shapes are normalised such that $\int_0^1 \Phi_j^2(x)\,\mathrm{d}x = 1$.

Finally, Equation (85) is recast under a quadratic DAE by introducing the velocities $v_j = \dot{q}_j$ as:

$$\dot{q}_j = v_j \tag{88}$$

$$\dot{v_j} = -\omega_j^2 q_j - \alpha T \sum_{k=1}^{N_{\text{mode}}} \Gamma_{jk} q_k \tag{89}$$

$$0 = T - \frac{1}{2} \sum_{k,l=1}^{N_{\text{mode}}} \Gamma_{kl}\ q_k q_l \tag{90}$$

For the numerical experiments, the first 15 linear transverse modes are used to discretise the continuous equation ($N_{\text{mode}} = 15$). After quadratic recast, this leads to a quadratic DAE with $N = 31$ variables in total (15 modal coordinates (q_j), 15 modal velocities (v_j) and 1 auxiliary variable (T)).

5.2 Reference Solution

In order to draw comparisons and assess the quality of the normal form results, a reference solution is computed for the first (transverse) vibration mode of the clamped clamped beam using a numerical HBM with 20 harmonics and the ANM for the continuation of the periodic solution, coded in the software Manlab [43].

The reference solution for the first bending mode exhibits a 1:5 internal resonance with the 3rd linear mode [55] located at frequency $\omega \simeq 1.1\omega_1$ on the backbone curve. This feature will not be captured with the normal form since we are only considering a single mode reduction in the application. Note however that the method proposed in this paper can be applied to capture the internal resonance by keeping more normal variables $z_3, z_4, \ldots$ in order to account for the resonant modes in the reduced dynamics [56, 28].

5.3 Example of normal form results

The normal forms for the first transverse mode of the clamped clamped beam are computed up to degree 35 and compared to the reference solution in Figure 11, where the modal amplitude q_1, q_3 and q_5 are depicted as a function of the natural angular frequency ω. As the degree of the normal form increases, the results get closer and closer to the reference solution. The modal amplitude of the coordinates q_3 and q_5 are well captured by the change of coordinates, and the evolution of the natural angular frequency is well evaluated by the reduced dynamics. Note however that, at a certain amplitude, the results start to diverge from the reference solution, and the divergence appears at lower amplitude for higher degree normal forms.

The effect of increasing the normal form degree is even clearer in Figure 12 where the relative error in angular frequency (between the normal form and the reference solution) is depicted. Increasing the degree of the normal form lowers the relative error by orders of magnitude, in the validity range of the series. However, at one point increasing the degree does not seem to have any effect on the error, indicating that moderate degree normal forms should be considered ($10 \leq D \leq 20$). One recovers the results presented in [27] in which the case of a

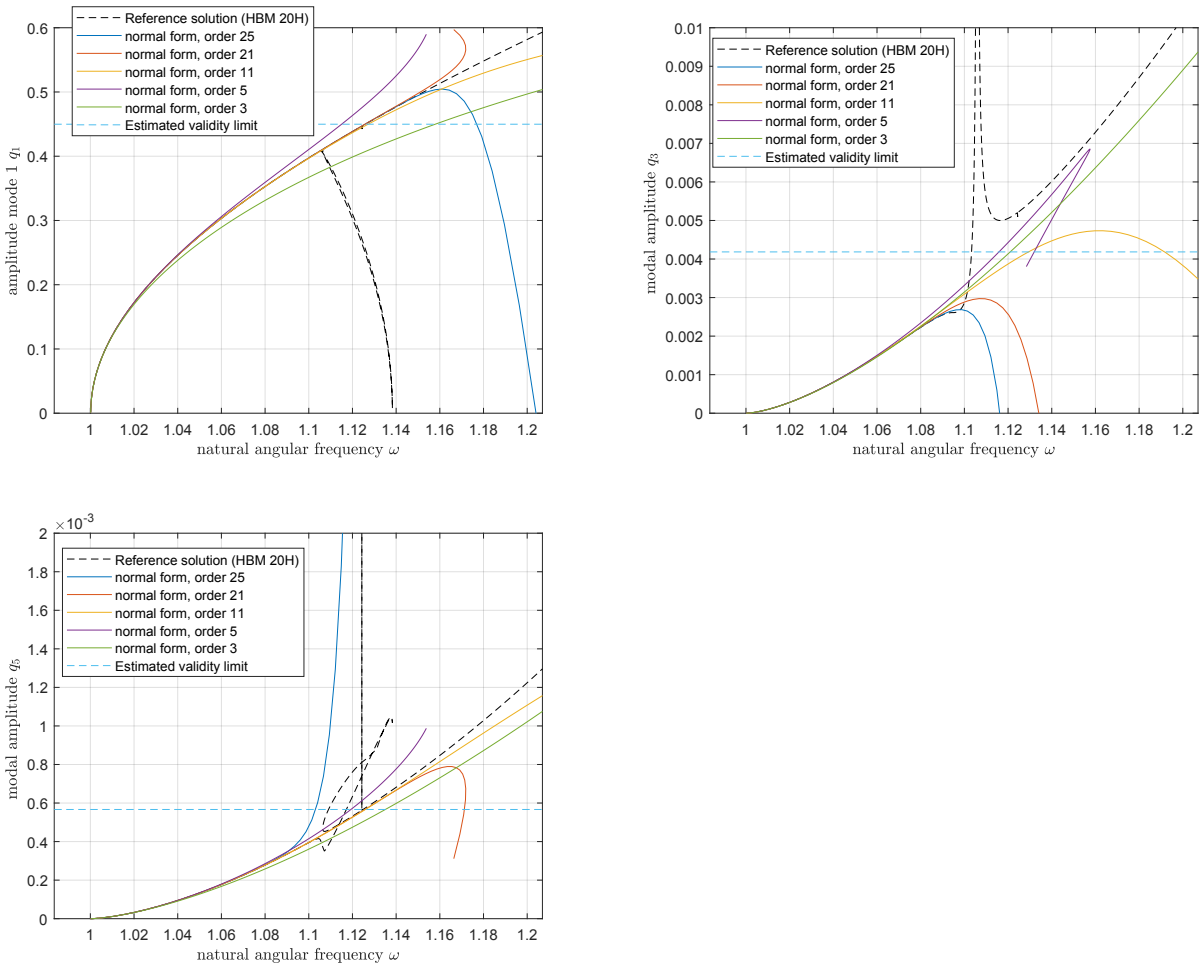

Figure 11: Comparison between the normal form backbone curves and the reference solution for the three modal amplitudes q_1, q_3 and q_5 as a function of the normalised angular frequency $\omega = \Omega/\omega_1$

clamped-clamped beam is considered with the same reduced-order modelling strategy but applied to a 3D finite element discretisation. In both cases, the validity limit of the order three normal form is for a normalised modal amplitude of $q_1 = 0.15$ (corresponding $\omega \simeq 1.01\omega_1$ on the backbone curve and to a vibration amplitude at the center of the beam equivalent to $0.15\Phi_1(1/2) = 0.24$ times the thickness of the beam), whereas an order five normal form is valid up to a normalised vibration amplitude of $q_1 = 0.3$ ($\omega \simeq 1.01\omega_1$ on the backbone curve and $0.3\Phi_1(1/2) = 0.48$ times the thickness for the vibration amplitude at the center of the beam). Our result also extend the results of [27] since our computations shows the validity limits of the various degrees of the normal form on a larger range of amplitude and frequency.

The validity limit of the normal form expansion can be estimated using the Cauchy or d'Alembert criterion presented in Section 2.5, and depicted in Figure 13. In this case, the Cauchy criterion appears to be more robust than the d'Alembert one, probably due to the small magnitudes of the coefficients appearing in the series at higher degree. One can see that the estimated validity limit based on the proposed criterion is in good agreement with qualitative and quantitative comparisons given in Figure 11 and Figure 12.

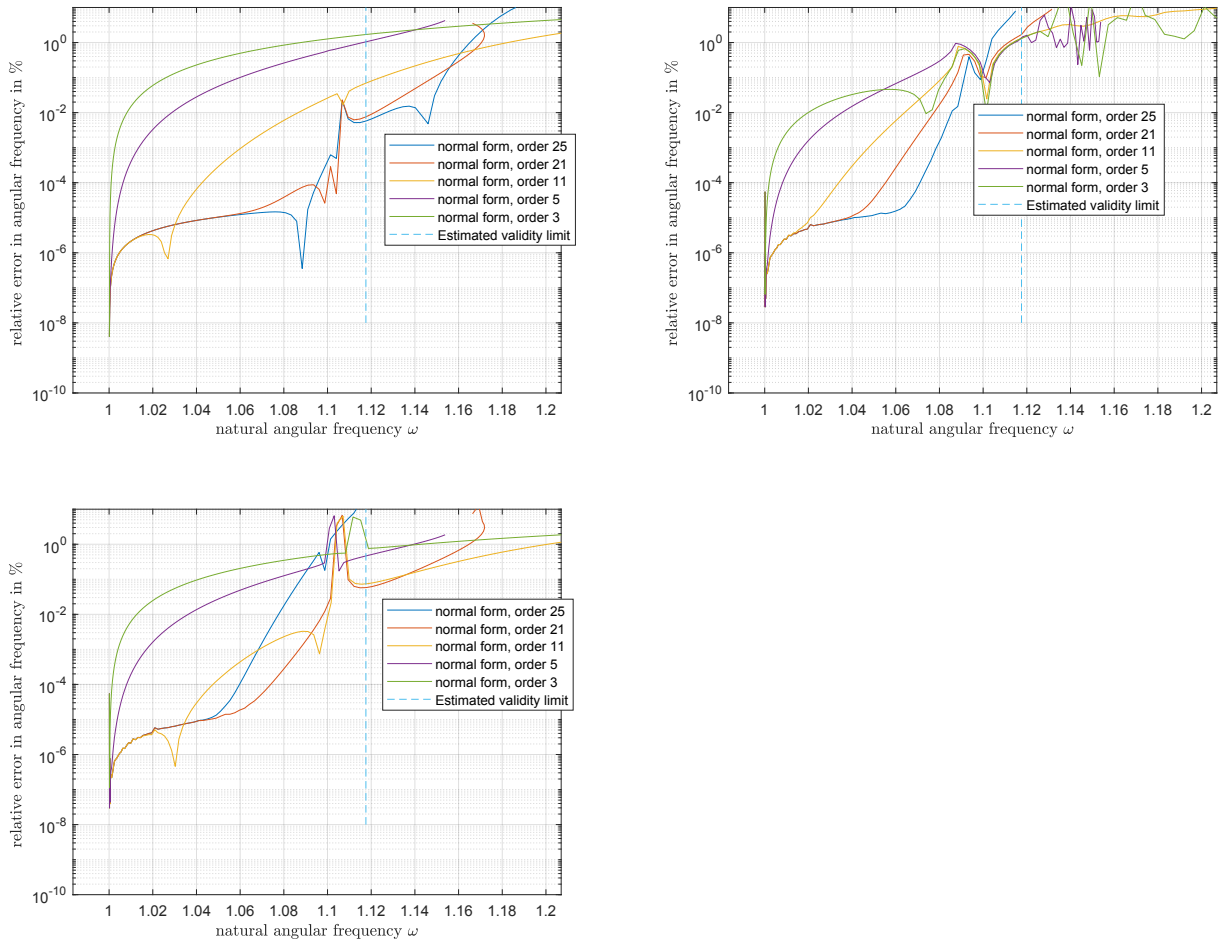

Figure 12: Relative error in angular frequency (as compared to the reference solution) for the three modal amplitudes q_1, q_3 and q_5 as a function of the normalised angular frequency $\omega = \Omega/\omega_1$

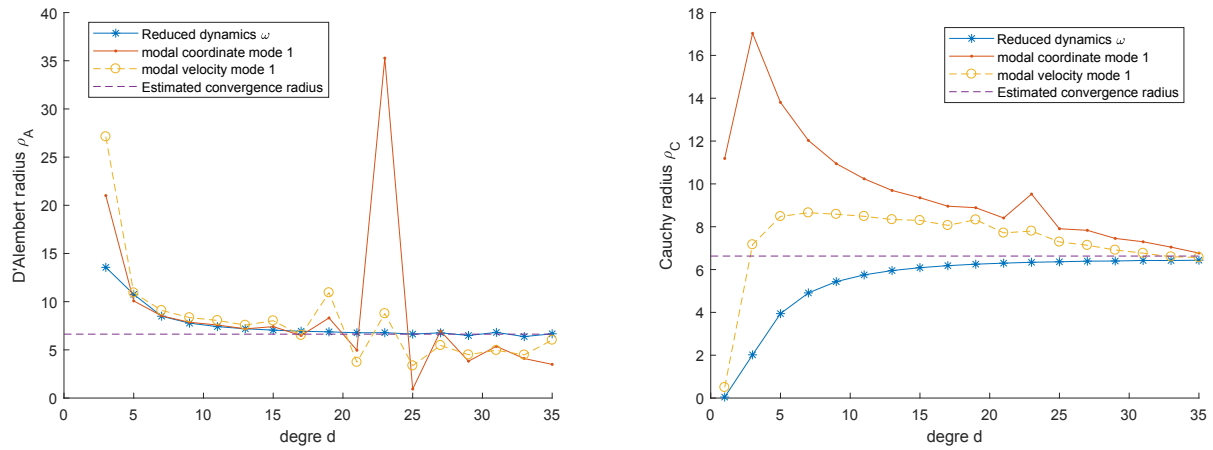

Figure 13: Clamped-clamped beam, convergence radius estimation as a function of the normal form degree using d'Alembert (left plot) or Cauchy (right plot) criteria

6 Cantilever Beam with geometrically exact finite-element model

As as final application example, we consider here a clamped-free beam discretised with a geometrically exact finite-element model. The aim of this example is to show that the proposed procedure can be applied to large quadratic DAE used to model mechanical structures. In what follows only a normal form with two variables will be considered, leading to the construction of a reduced model with a drastically reduced number of variables.

6.1 Description of the model

The model used here is a reformulation of the model proposed in [57, 46] and only the main developments are given in the following. We consider a straight clamped-free beam of length L with a homogeneous cross section of area S and second moment of area I, made out of an isotropic and homogeneous material. The axis of the beam is assumed to be initially aligned with the x axis. In the following, only the motion of the beam in the x, y plane will be considered (2D model).

Using a rigid body assumption for the displacement field of the cross section (Timoshenko kinematics), the motion of any point of the beam can be related to the displacement of the middle line and the position in the cross section in the undeformed configuration. In order to represent the rotation of the cross section, unitary complex numbers $a + ib$ are used to replace the usual rotation of the cross section [46, 57], denoted here by an angle $\psi(x,t)$, with $a = \cos\psi$ and $b = \sin\psi$. This allows to represent rotation as quadratic operations, instead of sine and cosine functions, at the price of including a constraint of the type $a^2 + b^2 = 1$ at each point of the middle line. Another solution would have been to use quaternions, as done in [58, 59]

The constraint is taken into account through the use of a Lagrange multiplier μ. The unknown vector field, denoted $U(x,t)$, can then be defined as:

$$U^T(x,t) = \begin{bmatrix} u(x,t) & v(x,t) & a(x,t) & b(x,t) & \mu(x,t) \end{bmatrix} \tag{91}$$

where u (resp. v) is the axial (resp. transverse) displacement of the centerline, a and b are the component of the complex number used to represent the rotation $\psi(x,t)$ of the cross section (i.e. $a = \cos\psi$ and $b = \sin\psi$) and μ is the Lagrange multiplier used to enforce the constraint $a^2 + b^2 = 1$ along the beam. $x \in [0,1]$ is the normalised location along the middle axis of the beam (i.e. $x = x^*/L$ with x^* the dimensioned location), t is the normalised time, $\circ' = \partial \circ /\partial x$, $\dot{\circ} = \partial \circ /\partial x$. The two displacement fields u and v are normalised with the length L of the beam, instead of using h for the clamped-clamped beam in section 5 (i.e. $(u,v) = (u^*, v^*)/L$ with (u^*, v^*) the dimensioned displacements). Using this scaling, it can be shown that the dynamics of the beam does depend mainly on one dimensionless parameter $\eta = I/(SL^2)$ and that if the beam is very slender, the effect of η on the backbone curve is negligible [60]. In this particular example we choose $\eta \approx 4.10^{-6}$.

The strain measure is based on a consistant linearisation of the full Green-Lagrange strain tensor (see e.g [57]) and can be written as:

$$e = (1 + u')a + v'b - 1 \tag{92}$$
$$\gamma = -(1 + u')b + v'a \tag{93}$$
$$\chi = ab' - a'b \tag{94}$$

where e is the axial strain, γ is the shear strain and χ is the curvature.

The beam is discretised with quadratic Timoshenko beam elements (with 3 nodes per element). At each node j, the dofs consist in the axial displacement u_j, the transverse displacement v_j, the two components of complex number (a_j, b_j) used to represent the rotation of the section, and the Lagrange multiplier μ_j. The nodal degrees of freedom are gathered in a vector z_j for $j = 1, 2, 3$ defined as:

$$z_j^T = \begin{bmatrix} u_j & v_j & a_j & b_j & \mu_j \end{bmatrix} \tag{95}$$

and the element degrees of freedom are gathered in a vector z defined as:

$$z^T = \begin{bmatrix} z_1^T & z_2^T & z_3^T \end{bmatrix} \tag{96}$$

The interpolation of the vector field over a single element can be written as:

$$U(x,t) = P(x)z(t), \tag{97}$$

where $P(x)$ is the interpolation matrix of size 5×15 defined as:

$$P(x) = \begin{bmatrix} N_1(x)I_5 & N_2(x)I_5 & N_3(x)I_5 \end{bmatrix}. \tag{98}$$

where I_5 is the identity matrix of dimension 5 and $N_1(s)$, $N_2(s)$ and $N_3(s)$ are the quadratic interpolation functions over the element.

For a single (quadratic) element the equation of motion for the 15 dof contained in the vector z can be written under the form:

$$M\ddot{z} = F_{int}(z)$$

where M is the element mass matrix and $F_{int}(x)$ is the vector of internal forces. The elementary internal forces are computed using the virtual work principle along with reduced Gauss integration to avoid shear locking [61]. Using a 2 points Gauss integration, the elementary vector of internal forces can be written as:

$$F_{int}(z) = \frac{L_e}{2}\left[Q(x_1)^T f_{int}(P(x_1)z) + Q(x_2)^T f_{int}(P(x_2)z)\right] \tag{99}$$

where the matrix $Q(x)$ is given by:

$$Q(x) = \begin{bmatrix} P(x) \\ \frac{dP}{dx}(x) \end{bmatrix} \tag{100}$$

where x_1, x_2 are the location of the Gauss points along the element, and f_{int} is defined by:

$$f_{int}^T(U) = \begin{bmatrix} 0 & 0 & -bT_2 & aT_2 & 0 & F_x & F_y & M_a + 2\mu a & M_b + 2\mu b & a^2 + b^2 - 1 \end{bmatrix} \tag{101}$$

where $N = ESe$, $T = GS\gamma$, $F_x = aN - bT$, $F_y = bN + aT$, $T_2 = N\gamma - (1+e)T$, $M_a = EIa'$ and $M_b = EIb'$.

The elementary force vector F_{int} will therefore depend quadratically on the values of the various fields $a, b, \mu, u', v', a', b', e, \gamma, T_2$ evaluated at the Gauss points. In this work, we choose to include an additional 20 auxiliary variables per Gauss point (40 auxiliary variables per elements) in order to render the expression of F_{int} linear with relation to those variables. This was also motivated for post-processing reasons as in this case one can directly access the results for the auxiliary variables (which have meaningful physical interpretation) instead of recomputing it from the displacement field.

For the complete beam, the elementary mass matrices and forces vectors are assembled over the whole structure and the system is put into the form of a quadratic DAE by adding auxiliary variables to the system. For the numerical application, the beam is discretised with $N_e = 30$ quadratic elements (3 nodes per element, with 5 dof per node). After quadratic recast and assembly, the final quadratic DAE contains $N = 1740$ variables in total (240 positions, 240 velocities, 60 Lagrange multipliers and 1200 auxiliary variables).

6.2 Reference solution

For this example, a reference solution is computed using the harmonic balance method with $H = 20$ harmonics. The Manlab package is used to compute the solution using the ANM. Note that the same input (the same quadratic DAE) is directly used as an input to compute the normal form.

6.3 Example of normal form results

The normal form for the first mode of the cantilever beam is computed for various degree $1 \leq D \leq 31$. The evolution of the natural angular frequency ω as a function of the normalised transverse amplitude of the free end $v(L)$ is depicted in Figure 14 and compared to the reference solution. One can observe a good agreement between the normal form solutions and the reference solutions. One can note that the normal form of degree 31 has a lower range of validity than the other, as it sharply changes direction when the amplitude reaches 0.5.

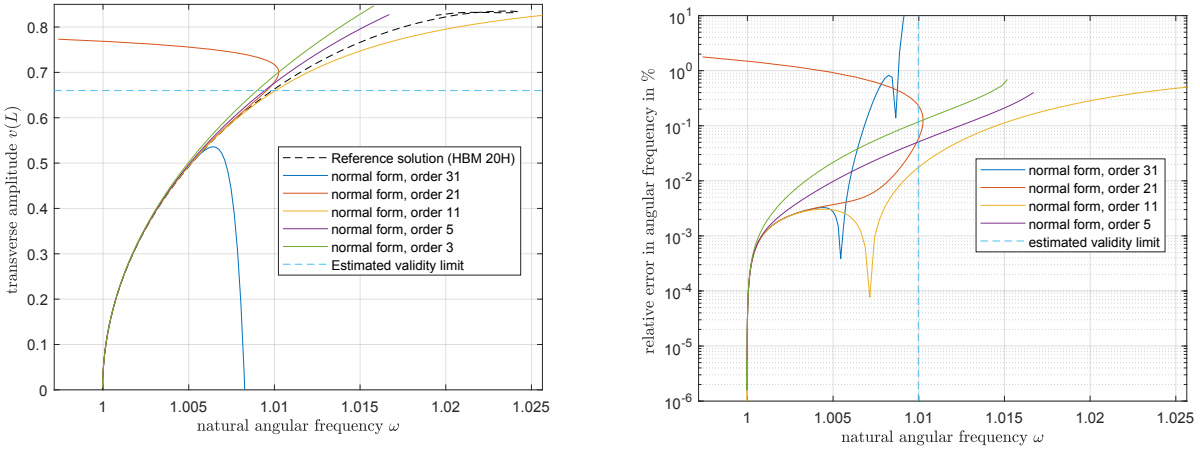

Figure 14: Left: Evolution of the fundamental angular frequency ω as a function of the transverse amplitude at the free end. Right: relative error in angular frequency for the normal form of the cantilever beam at various degree. Note the figures are plotted as a function of the normalised angular frequency $\omega = \Omega/\omega_1$

Figure 14 should be compared to Fig.5c of [27] where the authors computed a normal form for the clamped free beam problem using 3D finite element model (as opposed to a beam finite element model in the present paper). Even if the slenderness parameter of the studied beam are slightly different ($\eta \approx 4.16.10^{-6}$ in our case and $\eta \approx 1.16.10^{-6}$ in [27]), a very good agreement is observed between the results obtained from normal forms using a 3D model (Fig.5c of [27]) or using a beam model (Figure 14). In particular, the validity for the transverse displacement using a normal form at order 3 seems to be around the order of $0.5L$ in both cases.

The relative error in angular frequency $\epsilon = \frac{\omega_{\text{hbm}} - \omega_{\text{nf}}}{\omega_{\text{hbm}}}$ is depicted in Figure 14. One can see that for low angular frequency, all the normal form results are equivalent. However, the high degree (31) normal form quickly degrades in quality, whereas the normal form of moderate degree (11) has a relatively good global behaviour, and seems to be the best choice to make in this example.

To understand the previous results, we analyse the coefficients of the series (displacement v and reduced dynamics $\omega = \dot{\theta}$) to estimate the radius of convergence using the d'Alembert and the Cauchy criteria. The results are depicted in Figure 14. In both criteria, one can see that the convergence radius estimated using the reduced dynamics series shows a rapid convergence to a stable limit ($\rho^* \approx 1.6$). For the series associated to the displacement, using the d'Alembert criterion, the convergence radius first tend to the same as the reduced dynamics, but after a certain degree (here around 25) there is a sudden drop in the convergence radius, explaining the bad quality of the high degree normal form results at high amplitude. This might be due to numerical instabilities occurring during the computation as high degree, as the matrices start to be ill conditioned, and the coefficients of the series being very small. This might also be due to the fact that normal form are asymptotic expansions that start to degrade at high amplitude when increasing the number of terms in the series.

The radius of convergence estimated using the Cauchy coefficient seems to have a more monotonous convergence, but one can see that the validity limit estimated using the position $v(L)$ and $v(L/2)$ is clearly not converged. We recommend that one should therefore consider normal forms of moderate degree, as high degree normal forms can prove to be suboptimal.

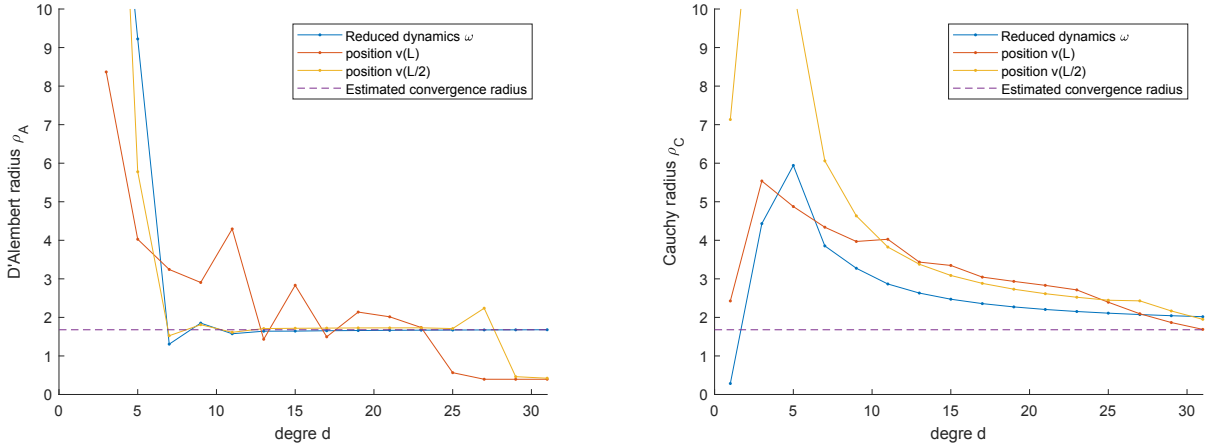

Figure 15: Evolution of the convergence radius estimated using the d'Alembert (left plot) or the Cauchy (right plot) coefficients as a function of the normal form degree.

The numerical instabilities for the coefficients of the change of variables at high degree seems to be confirmed if we look at the magnitude of the coefficients of the series as a function of the degree. Figure 16 depicts the evolutions of the modulus of the coefficients of various series as a function of the monomial number m. One can see that the amplitude of the coefficient is first decreasing, and is then re-increasing for monomial numbers greater than 350 (i.e for normal forms of degree greater than 25). Note that the series corresponding to the reduced dynamics $\omega = \dot{\theta}$ does however have a good behaviour as the modulus of the coefficients is strictly decreasing over the degree.

To give an estimation of the deformation of the beam, the vibration shape at the validity limit for the normal form is depicted in Figure 17.

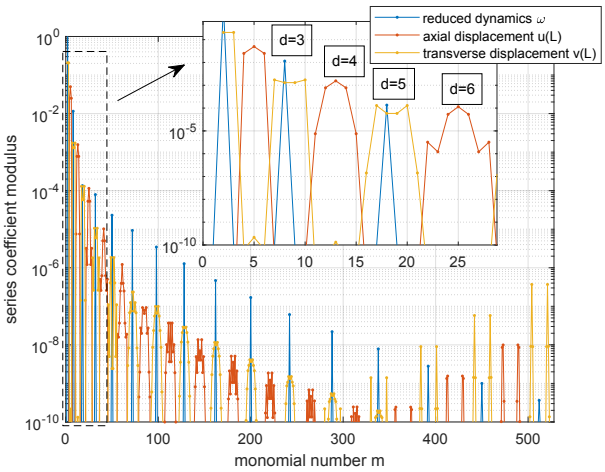

Figure 16: Modulus of the series coefficient for the reduced dynamics ω and the axial and transverse displacements at the free end of the beam as a function of the monomial number.

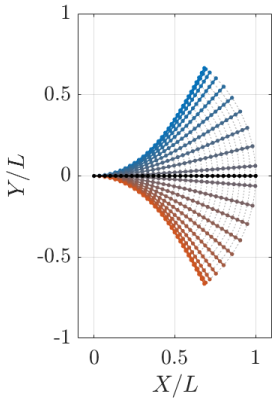

Figure 17: Vibration shape of the first mode of the cantilever beam at the quantitative validity limit amplitude of the normal form of degree 31

7 Conclusion

This paper considers the computation of normal forms for dynamic system written in the form of a quadratic differential equation, which is a general way of writing most of nonlinear systems encountered in various research an application fields. The normal form aims at finding a change of variable and reduced dynamics using polynomial expansion to carry out the computation. We propose here a method to write the (homological) equation to be solved at each degree based on linear algebra in the space of polynomials. This method allows for a general way of balancing the coefficients of each monomial in the homological equation, and can be easily coded. We also propose a criterion to evaluate the validity limit of the normal form based on d'Alembert and Cauchy criteria.

The proposed method is first applied in detail on a simple Duffing oscillator to illustrate the various matrices involved and the convergence results. The second example considers the case of a simple pendulum, and is here to illustrate the fact that the results of the normal form depends on the type of quadratic recast used to transform an original nonlinear system into a quadratic DAE. Finally, the method is applied to a larger system modelling a 2D cantilever beam using a geometrically exact finite-element. The results are in good agreement with the reference solution, but it shows that high degree normal form can lead to bad quality results at too high amplitude, and that moderate degree normal form should be used.

8 Acknowledgement

The authors would like to thank Pr Cyril Touzé and Pr Mathias Legrand for their valuable comments and remarks at multiple occasions and for their help in shaping the manuscript.

A Quadratic DAE with non zero equilibrium position

If the initial system contains a constant part C, then a lift is required to recast the variable around the origin to obtain a system under the form of Equation (1). Consider a system defined as:

$$A_C\dot{Y} = C + L_C Y + Q_C(Y, Y) \tag{102}$$

The static solution Y_s is defined by the algebraic equation:

$$0 = C + L_C Y_s + Q_C(Y_s, Y_s) \tag{103}$$

Using the change of variable $Y = Y_s + y$ (around a given stable static position Y_s), where y is now the new variable centred around origin, we obtain the following system of equation for y:

$$A_C\dot{y} = C + L_C(Y_s + y) + Q_C(Y_s + y, Y_s + y) \tag{104}$$

Using the definition of the equilibrium position Y_s, leads to

$$A_C\dot{y} = [L_C + Q_C(\cdot, Y_s) + Q_C(Y_s, \cdot)]\, y + Q_C(y, y) \tag{105}$$

which is identified as the quadratic DAE with zero equilibrium (1) where we have define $L = L_C + Q_C(\cdot, Y_s) + Q_C(Y_s, \cdot)$ (the tangent operator around the equilibrium) and $A = A_C$ and $Q = Q_C$.

B Polynomial algebra

B.1 Basis

We consider the space of polynomials with complex coefficients of degree D in n variables $z = (z_1, z_2, \ldots, z_n)$, denoted $\mathbb{C}_D[z]$. It is a vector space (over $\mathbb{C}$) with dimension $M = \frac{(D+n)!}{D!n!}$, the canonical monomial basis $B(z)$ is composed of the elementary monomials $b_m(z)$ given by:

$$b_m(z) = z^{\alpha_m} = z_1^{\alpha_{m1}}\ z_2^{\alpha_{m2}}\ \cdots\ z_n^{\alpha_{mn}} \tag{106}$$

with $\alpha_m = (\alpha_{m1}, \ldots, \alpha_{mn}) \in \mathbb{N}^n$ such that $|\alpha_m| \leq D$, for $m \in [0,\ M-1]$.

The elementary vector of the basis can be concatenated into the basis (column) vector $B(z)$ as:

$$B(z) = [b_0(z),\ b_1(z), \ldots, b_n(z), \ldots, b_{M-1}(z)]^T \tag{107}$$

In this paper, we sort the monomials of the basis by increasing total degree. In particular we set $b_0(z) = 1$ (the constant monomial, degree 0) , $b_1(z) = z_1$, $b_2(z) = z_2$, ..., and $b_n(z) = z_n$ (the linear monomials, degree 1) and so on. The basis $B(z)$ can be naturally split into $D+1$ families of monomials of constant degree. This leads to a special block structure for the derivation and multiplication matrices presented hereafter.

B.2 Derivation matrices

We consider a (column) vector of polynomials $W(z)$ expanded over the basis $B(z)$: $W(z) = WB(z)$. We consider the derivative operation ∂_{z_j} for $1 \leq j \leq N$ acting onto the vector $W(z)$, which can be written as follows:

$$\partial_{z_j} W(z) = W \partial_{z_j} B(z) \tag{108}$$

It can be seen that it is sufficient to know the effect of the derivation operation in the basis $\partial_{z_j} B(z)$ to compute the expression in the previous equation. If we consider a general monomial $b_m(z) = z^{\alpha^m} = z_1^{\alpha_1^m} \ldots z_n^{\alpha_n^m}$, then the derivation by z_j gives:

$$\partial_{z_j} b_m(z) = \alpha_j^m z_1^{\alpha_1^m} \cdots \times z_j^{\alpha_j^m - 1} \times \ldots z_n^{\alpha_n^m} = \alpha_j^m b_r(z) \tag{109}$$

where $b_r(z)$ is a given monomial of degree 1 less than $b_m(z)$. The results for all monomials can be gathered in a matrix ∇^j representing the operation ∂_{z_j} relative to the basis $B(z)$:

$$\partial_{z_j} B(z) = \nabla^j B(z) \tag{110}$$

where ∇^j is an $M \times M$ constant matrix of integers. The derivation operation ∂_{z_j} reduces the degree of the input polynomial by one, therefore the derivation matrices ∇^j are (block) lower triangular matrices (with blocs of zeros on the diagonal).

The derivative of a vector of polynomials can then be expressed as:

$$\partial_{z_j} W(z) = W \nabla^j B(z) \tag{111}$$

This relation simply states that the components of the derivative $\partial_{z_j} W(z)$ relative to the basis $B(z)$ are given by the matrix of coefficients $W\nabla^j$.

B.3 Multiplication matrices

We now consider the multiplication of a (column) vector of polynomials $W(z) = WB(z)$ by a scalar polynomial $\lambda(z) = \lambda B(z)$. The product can be expressed as:

$$\lambda(z)W(z) = \sum_{r=0}^{M-1} \sum_{s=0}^{M-1} \lambda_r W_s b_r(z) b_s(z) = W \sum_{r=0}^{M-1} \lambda_r b_r(z) B(z) \tag{112}$$

we see that only the products $b_r(z)B(z)$ are needed to compute the previous expression. We consider a general monomial product $b_r(z)b_s(z)$. If the degree of this product if less than the degree D, then it actually corresponds to another monomial of the basis, e.g. $b_m(z)$. If the degree of $b_r(z)b_s(z)$ is greater than D, then this term is out of the vector space $\mathbb{C}_D^N[z]$ and are discarded. The result can be summarized using a multiplication matrix defined as:

$$b_m(z)B(z) = \Delta^m B(z) \tag{113}$$

where Δ^m is an $M \times M$ constant Boolean matrix representing the operation "multiply by $b_m(z)$" relative to the basis $B(z)$. The product of $\lambda(z)W(z)$ can then be expressed as:

$$\lambda(z)W(z) = W \sum_{m=0}^{M-1} \lambda_m \Delta^m B(z) \tag{114}$$

B.4 Matrices for $n = 2$, $D = 3$

We give here the explicit expression for the derivation and multiplications matrices in the case of polynomials of degree $D = 3$ in $n = 2$ variables $z = (z_1, z_2)$. The vector space $\mathbb{C}_D[z]$ is of dimension $M = 10$ and is generated by the basis:

$$B(z) = \left[1,\ z_1,\ z_2,\ z_1^2,\ z_1 z_2,\ z_2^2,\ z_1^3,\ z_1^2 z_2,\ z_1 z_2^2,\ z_2^3\right]^T \tag{115}$$

B.4.1 Derivation matrices for $n = 2$, $D = 3$

The derivation matrices ∇^j (for j= 1, 2) are defined by:

$$\partial_{z_j} B(z) = \nabla^j B(z) \tag{116}$$

and are given by:

$$\nabla^1 = \left(\begin{array}{c|cc|ccc|cccc} 0 & 0 & 0 & 0 & 0 & 0 & 0 & 0 & 0 & 0 \\ \hline 1 & 0 & 0 & 0 & 0 & 0 & 0 & 0 & 0 & 0 \\ 0 & 0 & 0 & 0 & 0 & 0 & 0 & 0 & 0 & 0 \\ \hline 0 & 2 & 0 & 0 & 0 & 0 & 0 & 0 & 0 & 0 \\ 0 & 0 & 1 & 0 & 0 & 0 & 0 & 0 & 0 & 0 \\ 0 & 0 & 0 & 0 & 0 & 0 & 0 & 0 & 0 & 0 \\ \hline 0 & 0 & 0 & 3 & 0 & 0 & 0 & 0 & 0 & 0 \\ 0 & 0 & 0 & 0 & 2 & 0 & 0 & 0 & 0 & 0 \\ 0 & 0 & 0 & 0 & 0 & 1 & 0 & 0 & 0 & 0 \\ 0 & 0 & 0 & 0 & 0 & 0 & 0 & 0 & 0 & 0 \end{array}\right), \quad \nabla^2 = \left(\begin{array}{c|cc|ccc|cccc} 0 & 0 & 0 & 0 & 0 & 0 & 0 & 0 & 0 & 0 \\ \hline 0 & 0 & 0 & 0 & 0 & 0 & 0 & 0 & 0 & 0 \\ 1 & 0 & 0 & 0 & 0 & 0 & 0 & 0 & 0 & 0 \\ \hline 0 & 0 & 0 & 0 & 0 & 0 & 0 & 0 & 0 & 0 \\ 0 & 1 & 0 & 0 & 0 & 0 & 0 & 0 & 0 & 0 \\ 0 & 0 & 2 & 0 & 0 & 0 & 0 & 0 & 0 & 0 \\ \hline 0 & 0 & 0 & 0 & 0 & 0 & 0 & 0 & 0 & 0 \\ 0 & 0 & 0 & 1 & 0 & 0 & 0 & 0 & 0 & 0 \\ 0 & 0 & 0 & 0 & 2 & 0 & 0 & 0 & 0 & 0 \\ 0 & 0 & 0 & 0 & 0 & 3 & 0 & 0 & 0 & 0 \end{array}\right) \tag{117}$$

B.4.2 Multiplication matrices for $n = 2$, $D = 3$

The multiplication matrices Δ^m, for $m = 0,\ \ldots,\ M-1$, are defined by:

$$b_m(z)B(z) = \Delta^m B(z) \tag{118}$$

Constant and linear matrices

The matrix Δ^0 is the identity matrix of size M. The matrices Δ^1 and Δ^2 are given by:

$$\Delta^1 = \left(\begin{array}{c|ccc|ccc|cccc} 0 & 1 & 0 & 0 & 0 & 0 & 0 & 0 & 0 & 0 \\ \hline 0 & 0 & 0 & 1 & 0 & 0 & 0 & 0 & 0 & 0 \\ 0 & 0 & 0 & 0 & 1 & 0 & 0 & 0 & 0 & 0 \\ \hline 0 & 0 & 0 & 0 & 0 & 0 & 1 & 0 & 0 & 0 \\ 0 & 0 & 0 & 0 & 0 & 0 & 0 & 1 & 0 & 0 \\ 0 & 0 & 0 & 0 & 0 & 0 & 0 & 0 & 1 & 0 \\ \hline 0 & 0 & 0 & 0 & 0 & 0 & 0 & 0 & 0 & 0 \\ 0 & 0 & 0 & 0 & 0 & 0 & 0 & 0 & 0 & 0 \\ 0 & 0 & 0 & 0 & 0 & 0 & 0 & 0 & 0 & 0 \\ 0 & 0 & 0 & 0 & 0 & 0 & 0 & 0 & 0 & 0 \end{array}\right), \quad \Delta^2 = \left(\begin{array}{c|ccc|ccc|cccc} 0 & 0 & 1 & 0 & 0 & 0 & 0 & 0 & 0 & 0 \\ \hline 0 & 0 & 0 & 0 & 1 & 0 & 0 & 0 & 0 & 0 \\ 0 & 0 & 0 & 0 & 0 & 1 & 0 & 0 & 0 & 0 \\ \hline 0 & 0 & 0 & 0 & 0 & 0 & 0 & 1 & 0 & 0 \\ 0 & 0 & 0 & 0 & 0 & 0 & 0 & 0 & 1 & 0 \\ 0 & 0 & 0 & 0 & 0 & 0 & 0 & 0 & 0 & 1 \\ \hline 0 & 0 & 0 & 0 & 0 & 0 & 0 & 0 & 0 & 0 \\ 0 & 0 & 0 & 0 & 0 & 0 & 0 & 0 & 0 & 0 \\ 0 & 0 & 0 & 0 & 0 & 0 & 0 & 0 & 0 & 0 \\ 0 & 0 & 0 & 0 & 0 & 0 & 0 & 0 & 0 & 0 \end{array}\right) \tag{119}$$

Degree 2 matrices

The degree 2 multiplication matrices are given by:

$$\Delta^3 = \left(\begin{array}{c|ccc|ccc|cccc} 0 & 0 & 0 & 1 & 0 & 0 & 0 & 0 & 0 & 0 \\ \hline 0 & 0 & 0 & 0 & 0 & 0 & 1 & 0 & 0 & 0 \\ 0 & 0 & 0 & 0 & 0 & 0 & 0 & 1 & 0 & 0 \\ \hline 0 & 0 & 0 & 0 & 0 & 0 & 0 & 0 & 0 & 0 \\ 0 & 0 & 0 & 0 & 0 & 0 & 0 & 0 & 0 & 0 \\ 0 & 0 & 0 & 0 & 0 & 0 & 0 & 0 & 0 & 0 \\ \hline 0 & 0 & 0 & 0 & 0 & 0 & 0 & 0 & 0 & 0 \\ 0 & 0 & 0 & 0 & 0 & 0 & 0 & 0 & 0 & 0 \\ 0 & 0 & 0 & 0 & 0 & 0 & 0 & 0 & 0 & 0 \\ 0 & 0 & 0 & 0 & 0 & 0 & 0 & 0 & 0 & 0 \end{array}\right), \quad \Delta^4 = \left(\begin{array}{c|ccc|ccc|cccc} 0 & 0 & 0 & 0 & 1 & 0 & 0 & 0 & 0 & 0 \\ \hline 0 & 0 & 0 & 0 & 0 & 0 & 0 & 1 & 0 & 0 \\ 0 & 0 & 0 & 0 & 0 & 0 & 0 & 0 & 1 & 0 \\ \hline 0 & 0 & 0 & 0 & 0 & 0 & 0 & 0 & 0 & 0 \\ 0 & 0 & 0 & 0 & 0 & 0 & 0 & 0 & 0 & 0 \\ 0 & 0 & 0 & 0 & 0 & 0 & 0 & 0 & 0 & 0 \\ \hline 0 & 0 & 0 & 0 & 0 & 0 & 0 & 0 & 0 & 0 \\ 0 & 0 & 0 & 0 & 0 & 0 & 0 & 0 & 0 & 0 \\ 0 & 0 & 0 & 0 & 0 & 0 & 0 & 0 & 0 & 0 \\ 0 & 0 & 0 & 0 & 0 & 0 & 0 & 0 & 0 & 0 \end{array}\right), \tag{120}$$

$$\Delta^5 = \left(\begin{array}{c|ccc|ccc|cccc} 0 & 0 & 0 & 0 & 0 & 1 & 0 & 0 & 0 & 0 \\ \hline 0 & 0 & 0 & 0 & 0 & 0 & 0 & 0 & 1 & 0 \\ 0 & 0 & 0 & 0 & 0 & 0 & 0 & 0 & 0 & 1 \\ \hline 0 & 0 & 0 & 0 & 0 & 0 & 0 & 0 & 0 & 0 \\ 0 & 0 & 0 & 0 & 0 & 0 & 0 & 0 & 0 & 0 \\ 0 & 0 & 0 & 0 & 0 & 0 & 0 & 0 & 0 & 0 \\ \hline 0 & 0 & 0 & 0 & 0 & 0 & 0 & 0 & 0 & 0 \\ 0 & 0 & 0 & 0 & 0 & 0 & 0 & 0 & 0 & 0 \\ 0 & 0 & 0 & 0 & 0 & 0 & 0 & 0 & 0 & 0 \\ 0 & 0 & 0 & 0 & 0 & 0 & 0 & 0 & 0 & 0 \end{array}\right) \tag{121}$$

Degree 3 matrices

And finally the degree 3 multiplication matrices are given by:

$$\Delta^6 = \left(\begin{array}{c|ccc|ccc|cccc} 0 & 0 & 0 & 0 & 0 & 0 & 1 & 0 & 0 & 0 \\ \hline 0 & 0 & 0 & 0 & 0 & 0 & 0 & 0 & 0 & 0 \\ 0 & 0 & 0 & 0 & 0 & 0 & 0 & 0 & 0 & 0 \\ \hline 0 & 0 & 0 & 0 & 0 & 0 & 0 & 0 & 0 & 0 \\ 0 & 0 & 0 & 0 & 0 & 0 & 0 & 0 & 0 & 0 \\ 0 & 0 & 0 & 0 & 0 & 0 & 0 & 0 & 0 & 0 \\ \hline 0 & 0 & 0 & 0 & 0 & 0 & 0 & 0 & 0 & 0 \\ 0 & 0 & 0 & 0 & 0 & 0 & 0 & 0 & 0 & 0 \\ 0 & 0 & 0 & 0 & 0 & 0 & 0 & 0 & 0 & 0 \\ 0 & 0 & 0 & 0 & 0 & 0 & 0 & 0 & 0 & 0 \end{array}\right), \quad \Delta^7 = \left(\begin{array}{c|ccc|ccc|cccc} 0 & 0 & 0 & 0 & 0 & 0 & 0 & 1 & 0 & 0 \\ \hline 0 & 0 & 0 & 0 & 0 & 0 & 0 & 0 & 0 & 0 \\ 0 & 0 & 0 & 0 & 0 & 0 & 0 & 0 & 0 & 0 \\ \hline 0 & 0 & 0 & 0 & 0 & 0 & 0 & 0 & 0 & 0 \\ 0 & 0 & 0 & 0 & 0 & 0 & 0 & 0 & 0 & 0 \\ 0 & 0 & 0 & 0 & 0 & 0 & 0 & 0 & 0 & 0 \\ \hline 0 & 0 & 0 & 0 & 0 & 0 & 0 & 0 & 0 & 0 \\ 0 & 0 & 0 & 0 & 0 & 0 & 0 & 0 & 0 & 0 \\ 0 & 0 & 0 & 0 & 0 & 0 & 0 & 0 & 0 & 0 \\ 0 & 0 & 0 & 0 & 0 & 0 & 0 & 0 & 0 & 0 \end{array}\right) \tag{122}$$

$$\Delta^8 = \left(\begin{array}{c|cc|ccc|cccc} 0 & 0 & 0 & 0 & 0 & 0 & 0 & 0 & 1 & 0 \\ \hline 0 & 0 & 0 & 0 & 0 & 0 & 0 & 0 & 0 & 0 \\ 0 & 0 & 0 & 0 & 0 & 0 & 0 & 0 & 0 & 0 \\ \hline 0 & 0 & 0 & 0 & 0 & 0 & 0 & 0 & 0 & 0 \\ 0 & 0 & 0 & 0 & 0 & 0 & 0 & 0 & 0 & 0 \\ 0 & 0 & 0 & 0 & 0 & 0 & 0 & 0 & 0 & 0 \\ \hline 0 & 0 & 0 & 0 & 0 & 0 & 0 & 0 & 0 & 0 \\ 0 & 0 & 0 & 0 & 0 & 0 & 0 & 0 & 0 & 0 \\ 0 & 0 & 0 & 0 & 0 & 0 & 0 & 0 & 0 & 0 \\ 0 & 0 & 0 & 0 & 0 & 0 & 0 & 0 & 0 & 0 \end{array}\right) \quad \Delta^9 = \left(\begin{array}{c|cc|ccc|cccc} 0 & 0 & 0 & 0 & 0 & 0 & 0 & 0 & 0 & 1 \\ \hline 0 & 0 & 0 & 0 & 0 & 0 & 0 & 0 & 0 & 0 \\ 0 & 0 & 0 & 0 & 0 & 0 & 0 & 0 & 0 & 0 \\ \hline 0 & 0 & 0 & 0 & 0 & 0 & 0 & 0 & 0 & 0 \\ 0 & 0 & 0 & 0 & 0 & 0 & 0 & 0 & 0 & 0 \\ 0 & 0 & 0 & 0 & 0 & 0 & 0 & 0 & 0 & 0 \\ \hline 0 & 0 & 0 & 0 & 0 & 0 & 0 & 0 & 0 & 0 \\ 0 & 0 & 0 & 0 & 0 & 0 & 0 & 0 & 0 & 0 \\ 0 & 0 & 0 & 0 & 0 & 0 & 0 & 0 & 0 & 0 \\ 0 & 0 & 0 & 0 & 0 & 0 & 0 & 0 & 0 & 0 \end{array}\right) \tag{123}$$

C Pendulum equation

C.1 Cartesian parametrisation

When $n = 1$ ($T_1(x) = x$), one recovers the equation of motion using Cartesian coordinates. If one sets $p_0 = \cos\theta = -y$ and $p_3 = \sin\theta = x$, then Equation (71) can be written as:

$$\ddot{y} + 1 = 2\lambda y \tag{124}$$
$$\ddot{x} = 2\lambda x \tag{125}$$
$$x^2 + y^2 - 1 = 0 \tag{126}$$

which are the classic equations for the pendulum (λ being the the tension in the rod). Note that the equation of motion is already in the form of a quadratic DAE.

C.2 Quaternion-like parametrisation

When $n = 2$ ($T_2(x) = 2x^2 - 1$), one recovers the equation of motion using "quaternion-like" parametrisation for the rotation of the pendulum. If one sets $p_0 = \cos\frac{\theta}{2}$ and $p_3 = \sin\frac{\theta}{2}$, then Equation (71) can be written as:

$$\ddot{p}_0 - p_0 = \frac{1}{2}\lambda p_0 \tag{127}$$
$$\ddot{p}_3 = \frac{1}{2}\lambda p_3 \tag{128}$$
$$p_0^2 + p_3^2 - 1 = 0 \tag{129}$$

which is in the form of a quadratic DAE.

Note that another form of the equations of motion is available in this case. Indeed, one can also write the potential energy as $U = p_3^2 - p_0^2$, resulting in a somehow more "symmetric" system of equations given by the following:

$$\ddot{p}_0 - \frac{1}{2}p_0 = \frac{1}{2}\lambda p_0 \tag{130}$$
$$\ddot{p}_3 + \frac{1}{2}p_3 = \frac{1}{2}\lambda p_3 \tag{131}$$
$$p_0^2 + p_3^2 - 1 = 0 \tag{132}$$

C.3 Parametrisation for $n \geq 3$

To illustrate the quadratic recast procedure, we consider the case $n = 4$ (the case $n = 3$ still leads to a quadratic DAE and needs no quadratic recast). For $n = 4$, the variables are defined as $p_0 = \cos\frac{\theta}{4}$ and $p_3 = \sin\frac{\theta}{4}$, and the resulting equations of motion are given by the following:

$$\begin{aligned} \ddot{p}_0 - 2p_0^3 + p_0 &= \frac{1}{8}\lambda p_0 \\ \ddot{p}_3 &= \frac{1}{8}\lambda p_3 \\ p_0^2 + p_3^2 - 1 &= 0 \end{aligned} \tag{133}$$

These equations are cubic (w.r.t. p_0) and the quadratic recast is done by introducing an auxiliary variable defined as $a = p_0^2$ so that the system takes the following quadratic DAE form:

$$\begin{aligned} \ddot{p}_0 - 2ap_0 + p_0 &= \frac{1}{8}\lambda p_0 \\ \ddot{p}_3 &= \frac{1}{8}\lambda p_3 \\ p_0^2 + p_3^2 - 1 &= 0 \\ a - p_0^2 &= 0 \end{aligned} \tag{134}$$

References

[1] H. Poincaré. *Les méthodes nouvelles de la mécanique céleste*. Gauthiers-Villars, Paris, 1892.

[2] V. I. Arnold. *Geometrical Methods in the Theory of Ordinary Differential Equations*. Springer, 1988.

[3] G. Iooss and M. Adelmeyer. *Topics in bifurcation theory*. World scientific, New-York, 1998. second edition.

[4] J. Murdock. *Normal forms and unfoldings for local dynamical systems*. Springer monographs in Mathematics, New-York, 2003.

[5] P. B. Kahn and Y. Zarmi. *Nonlinear Dynamics: Exploration Through Normal Forms*. Dover Books on Physics, 2014.

[6] M. Haragus and G. Iooss. *Local bifurcations, center manifolds, and normal forms in infinite dimensional systems*. EDP Science, 2009.

[7] S. Shaw and C. Pierre. Nonlinear normal modes and invariant manifolds. *Journal of Sound and Vibration*, 150(1):170–173, 1991.

[8] C. Touzé, O. Thomas, and A. Chaigne. Hardening/softening behaviour in non-linear oscillations of structural systems using non-linear normal modes. *Journal of Sound and Vibration*, 273(1-2):77–101, 2004.

[9] G. Haller and S. Ponsioen. Nonlinear normal modes and spectral submanifolds: existence, uniqueness and use in model reduction. *Nonlinear Dynamics*, 86:1493–1534, 2016.

[10] R.M. Rosenberg. The normal modes of nonlinear n-degree-of-freedom systems. *Journal of Applied Mechanics*, 29(1):7–14, 1962.

[11] G. Kerschen, M. Peeters, J.C. Golinval, and A.F. Vakakis. Nonlinear normal modes, Part I: A useful framework for the structural dynamicist. *Mechanical Systems and Signal Processing*, 23:170–194, 2009.

[12] A.M. Lyapunov. Probl'eme général de la stabilité du mouvement. *Annales de la faculté des sciences de Toulouse*, Série 2,9:203–474, 1907.

[13] A. Kelley. On the liapunov subcenter manifold. *Journal of Mathematical Analysis and Applications*, 18:472–478, 1967.

[14] R. de la Llave and F. Kogelbauer. Global persistence of lyapunov subcenter manifolds as spectral submanifolds under dissipative perturbations. *SIAM Journal of Applied Dynamical Systems*, 18(4):2099–2142, 2019.

[15] C. Touzé and M. Amabili. Nonlinear normal modes for damped geometrically nonlinear systems: Application to reduced-order modelling of harmonically forced structures. *Journal of Sound and Vibration*, 298(4-5):958–981, 2006.

[16] M. Krack. Nonlinear modal analysis of nonconservative systems: Extension of the periodic motion concept. *Computers and Structures*, 154:59–71, 2015.

[17] D. Laxalde and F. Thouverez. Complex non-linear modal analysis for mechanical systems: Application to turbomachinery bladings with friction interfaces. *Journal of Sound and Vibration*, 322(4–5):1009–1025, 2009.

[18] L. Jézéquel and C. H. Lamarque. Analysis of non-linear dynamical systems by the normal form theory. *Journal of Sound and Vibration*, 149(3):429–459, 1991.

[19] C. Touzé, O. Thomas, and A. Huberdeau. Asymptotic non-linear normal modes for large amplitude vibrations of continuous structures. *Computers and Structures*, 82(31-32):2671–2682, 2004.

[20] S. W. Shaw and C. Pierre. Normal modes of vibration for non-linear continuous systems. *Journal of Sound and Vibration*, 169:319–347, 1994.

[21] C. Touzé, A. Vizzaccaro, and O. Thomas. Model order reduction methods for geometrically nonlinear structures: a review of nonlinear techniques. *Nonlinear Dynamics*, 105:1141–1190, 2021.

[22] A. Opreni, A. Vizzaccaro, A. Martin, A. Frangi, and C. Touzé. Morfe project: Model order reduction for finite element structures, 2022.

[23] S. Jain, T. Thurnher, M. Li, and G. Haller. Computation of invariant manifolds and their reduced dynamics in high-dimensional mechanics problems, 2021.

[24] S. Ponsioen, T. Pedergnana, and G. Haller. Automated computation of autonomous spectral submanifolds for nonlinear modal analysis. *Journal of Sound and Vibration*, 420:269 – 295, 2018.

[25] S. Jain and G. Haller. How to compute invariant manifolds and their reduced dynamics in high-dimensional finite-element models. *Nonlinear Dynamics*, 107:1417–1450, 2022.

[26] A. Vizzaccaro, Y. Shen, L. Salles, J. Blahos, and C. Touzé. Direct computation of nonlinear mapping via normal form for reduced-order models of finite element nonlinear structures. *Computer Methods in Applied Mechanics and Engineering*, 284:113957, 2021.

[27] A. Vizzaccaro, A. Opreni, L. Salles, A. Frangi, and C. Touzé. High order direct parametrisation of invariant manifolds for model order reduction of finite element structures: application to large amplitude vibrations and uncovering of a folding point. *Nonlinear Dynamics*, 110(1):525–571, 2022.

[28] A. Opreni, A. Vizzaccaro, A. Frangi, and C. Touzé. Model order reduction based on direct normal form: application to large finite element MEMS structures featuring internal resonance. *Nonlinear Dynamics*, 105:1237–1272, 2021.

[29] A. Martin, A. Opreni, A. Vizzaccaro, M. Debeurre, L. Salles, A. Frangi, O. Thomas, and C. Touzé. Reduced order modeling of geometrically nonlinear rotating structures using the direct parametrisation of invariant manifolds. *Journal of Theoretical, Computational and Applied Mechanics (JTCAM)*, 10430, 2023.

[30] M. Li, S. Jain, and G. Haller. Nonlinear analysis of forced mechanical systems with internal resonance using spectral submanifolds – part I: Periodic response and forced response curve. *Nonlinear Dynamics*, 110:1005–1043, 2022.

[31] A. Opreni, A. Vizzaccaro, C. Touzé, and A. Frangi. High-order direct parametrisation of invariant manifolds for model order reduction of finite element structures: application to generic forcing terms and parametrically excited systems. *Nonlinear Dynamics*, 111:5401–5447, 2023.

[32] A. Vizzaccaro, G. Gobat, A. Frangi, and C. Touzé. Direct parametrisation of invariant manifolds for forced non-autonomous systems including superharmonic resonances. *Nonlinear Dynamics*, 2024.

[33] X. Cabré, E. Fontich, and R. de la Llave. The parameterization method for invariant manifolds. I. Manifolds associated to non-resonant subspaces. *Indiana Univ. Math. J.*, 52(2):283–328, 2003.

[34] X. Cabré, E. Fontich, and R. de la Llave. The parameterization method for invariant manifolds. II. Regularity with respect to parameters. *Indiana Univ. Math. J.*, 52(2):329–360, 2003.

[35] X. Cabré, E. Fontich, and R. de la Llave. The parameterization method for invariant manifolds. III. Overview and applications. *J. Differential Equations*, 218(2):444–515, 2005.

[36] A. Haro and R. de la Llave. A parameterization method for the computation of invariant tori and their whiskers in quasi-periodic maps: numerical algorithms. *Discrete and Continuous Dynamical Systems-B*, 6(6):1261, 2006.

[37] S. W. Shaw and C. Pierre. Normal modes for non-linear vibratory systems. *Journal of Sound and Vibration*, 164:85–124, 1993.

[38] T. Flament, J.-F. Deü, A. Placzek, M. Balmaseda, and D.-M. Tran. Reduced order model of nonlinear structures for turbomachinery aeroelasticity. *Journal of Engineering for Gas Turbines and Power*, 146:031005, 2024.

[39] J. Gonzalez, J.D. Mireles James, and N. Tuncer. Finite element approximation of invariant manifolds by the parameterization method. *Partial Differential Equations and Applications*, 3:75, 2022.

[40] L. Guillot, B. Cochelin, and C. Vergez. A generic and efficient Taylor series-based continuation method using a quadratic recast of smooth nonlinear systems. *International Journal for Numerical Methods in Engineering*, 119(4):261–280, 2019.

[41] L. Guillot, A. Lazarus, O. Thomas, C. Vergez, and B. Cochelin. A purely frequency based Floquet-Hill formulation for the efficient stability computation of periodic solutions of ordinary differential systems. *Journal of Computational Physics*, 416, 2020.

[42] A. Bychkov and G. Pogudin. Optimal monomial quadratization for ode systems. In *Combinatorial Algorithms. IWOCA 2021. Lecture Notes in Computer Science*, volume 12757. Springer, 2021.

[43] L. Guillot, A. Lazarus, O. Thomas, C. Vergez, and B. Cochelin. Manlab 4.0: an interactive path-following and bifurcation analysis software. Technical report, Laboratoire de Mécanique et d'Acoustique, CNRS, http://manlab.lma.cnrs-mrs.fr, 2018.

[44] A. Borri, F. Carravetta, and P. Palumbo. Quadratized taylor series methods for ode numerical integration. *Applied Mathematics and Computation*, 458:128237, 2023.

[45] M. Li, J. Shobhit, and G. Haller. Model reduction for constrained mechanical systems via spectral submanifolds. *Nonlinear Dynamics*, 111:8881–8911, 2023.

[46] M. Debeurre, A. Grolet, B. Cochelin, and O. Thomas. Finite element computation of nonlinear modes and frequency response of geometrically exact beam structures. *Journal of Sound and Vibration*, 548(117534), 2023.

[47] B. Wang, X. Kestelyn, E. Kharazian, and A. Grolet. Application of Normal Form Theory to Power Systems: A Proof of Concept of a Novel Structure-Preserving Approach. *IEEE Power and Energy Society General Meeting (PESGM)*, 2024.

[48] C. H. Lamarque, C. Touzé, and O. Thomas. An upper bound for validity limits of asymptotic analytical approaches based on normal form theory. *Nonlinear Dynamics*, 70(3):1931–1949, 2012.

[49] A.K. Stoychev and U.J. R"omer. Failing parametrizations: what can go wrong when approximating spectral submanifolds. *Nonlinear Dynamics*, 111:5963–6000, 2023.

[50] A. Giorgilli. *Notes on Hamiltonian Dynamical Systems*. Cambridge University Press, 2022.

[51] W. Rudin. *Principles Of Mathematical Analysis*. Mc Graw Hill, 1976.

[52] L. Guillot, A. Lazarus, O. Thomas, C. Vergez, and B. Cochelin. A purely frequency based Floquet-Hill formulation for the efficient stability computation of periodic solutions of ordinary differential systems. *Journal of Computational Physics*, 416:109477, 2020.

[53] H. Alvaro, E. Jairo, and H. Castillo. Exact solution to Duffing equation and the pendulum equation. *Applied Mathematical Sciences*, 8:8781–8789, 2014.

[54] R. Lewandowski. Solutions With Bifurcation Points For Free Vibration Of Beams: An Analytical Approach. *Journal of Sound and Vibration*, 177 (2):239–249, 1994.

[55] A. Givois, A. Grolet, O. Thomas, and J.-F. Deü. On the frequency response computation of geometrically nonlinear flat structures using reduced-order finite element models. *Nonlinear Dynamics*, 97(2):1747–1781, 2019.

[56] G. Gobat, L. Guillot, A. Frangi, B. Cochelin, and C. Touzé. Backbone curves, Neimark-Sacker boundaries and appearance of quasi-periodicity in nonlinear oscillators: Application to 1:2 internal resonance and frequency combs in MEMS. *Meccanica*, 56(8):1937–1969, August 2021.

[57] O. Thomas, A. Sénéchal, and J. F. Deü. Hardening/softening behaviour and reduced order modelling of nonlinear vibrations of rotating cantilever beams. *Nonlinear Dynamics*, 86(2):1293–1318, 2016.

[58] M. Debeurre, A. Grolet, and O. Thomas. Quaternion-based finite element computation of nonlinear modes and frequency responses of geometrically exact beam structures in three dimensions. *Multibody System Dynamics*, 2024. submitted.

[59] E. Cottanceau, O. Thomas, P. Véron, M. Alochet, and R. Deligny. A finite element/quaternion/asymptotic numerical method for the 3D simulation of flexible cables. *Finite Elements in Analysis and Design*, 139:14–34, 2018.

[60] M. Debeurre, A. Grolet, and O. Thomas. Extreme nonlinear dynamics of cantilever beams: effect of gravity and slenderness on the nonlinear modes. *Nonlinear Dynamics*, 111:12787–12815, 2023.

[61] A. Cardona and M. Géradin. A beam finite element non-linear theory with finite rotations. *International Journal for Numerical Methods in Engineering*, 26:2403–2438, 1988.